

# Empirical stream thermal sensitivities cluster on the landscape according to geology and climate

Lillian M. McGill<sup>1</sup>, E. Ashley Steel<sup>2</sup>, Aimee H. Fullerton<sup>3</sup>

<sup>1</sup>Center for Quantitative Sciences, University of Washington, Seattle, WA 98105, USA, ORCID ID: 0000-0003-2722-2917

<sup>2</sup>School of Aquatic and Fishery Sciences, University of Washington, Seattle, WA 98105, USA, ORCID ID: 0000-0001-5091-276X

<sup>3</sup>Northwest Fisheries Science Center, National Oceanic and Atmospheric Administration, 2725 Montlake Blvd. East, Seattle, WA 98112, USA, ORCID 0000-0002-5581-3434

*Correspondence to:* Lillian M. McGill (lmcgill@uw.edu)

## Abstract

Climate change is modifying river temperature regimes across the world. To apply management interventions in an effective and efficient fashion, it is critical to both understand the underlying processes causing stream warming and identify the streams most and least sensitive to environmental change. Empirical stream thermal sensitivity, defined as the change in water temperature with a single degree change in air temperature, is a useful tool to characterize historical stream temperature conditions and to predict how streams might respond to future climate warming. We measured air and stream temperature across the Snoqualmie and Wenatchee basins, Washington during hydrologic years 2015-2021. We used ordinary least squares regression to calculate seasonal summary metrics of thermal sensitivity and time-varying coefficient models to derive continuous estimates of thermal sensitivity for each site. We then applied classification approaches to determine unique thermal sensitivity regimes and, further, to establish a link between environmental covariates and thermal sensitivity regime. We found a diversity of thermal sensitivity responses across our basins that differed in both timing and magnitude of sensitivity. We also found that covariates describing underlying geology and snowmelt were the most important in differentiating clusters. Our findings and our approach can be used to inform strategies for river basin restoration and conservation in the context of climate change, such as identifying climate insensitive areas of the basin that should be preserved and protected.

## 1 Introduction

Globally, river temperature regimes are shifting in response to a changing climate. As water temperature is a critical component of aquatic ecosystems, these changes will alter an essential element of the habitat of many lotic organisms (Daufresne and Boët 2007). To apply management interventions in an effective and efficient fashion, it is critical to both understand the underlying processes causing stream warming (Arismendi et al. 2014, Steel et al. 2017) and identify the streams most and least sensitive to environmental change (Parkinson et al. 2016, Pyne and Poff 2017, Jackson et al. 2018). Measures of empirical stream thermal sensitivity, defined as the change in water temperature

34 with a single degree change in air temperature, or the slope of the statistical relationship between air temperature and  
35 water temperature, address both concerns.

36 Thermal sensitivities reflect the combined influence of both spatially and temporally varying meteorological  
37 and hydrological factors, and a large body of literature examines hypothesized climate, landscape, and hydrogeologic  
38 drivers of thermal sensitivity (Table 1A). Variation in solar radiation is often the most important driver of both air and  
39 river temperature, and as a result, air and river temperatures are typically correlated (Johnson 2003, Leach et al. 2023).  
40 Landscape features such as riparian canopy cover and topographic shading associated with steep watersheds can  
41 reduce exposure to solar radiation, suppressing stream temperatures (Webb and Zhang 1997). Stream temperature is  
42 also influenced by discharge through changes to thermal inertia and residence time (Meier et al. 2003) and runoff  
43 composition where snowmelt, surface runoff, or groundwater inflow entering the stream have different temperature  
44 signatures than the stream itself (Webb and Zhang 1997, Mohseni and Stefan 1999, Cadbury et al. 2008). Inputs from  
45 water sources such as snowmelt and groundwater upwelling decouple air and water temperatures and result in a  
46 decreased thermal sensitivity of water temperature to air temperature (Tague et al. 2007, Mayer 2012, Johnson et al.  
47 2014). As a result, the relationship between air and water temperature can also be a useful diagnostic tool for  
48 identifying putative hydrological processes for which empirical measures are often unavailable. Thermal sensitivity  
49 has been used in the past to estimate areas of shallow and deep groundwater influence (Snyder et al. 2015, Briggs et  
50 al. 2018) and understand the role of snowmelt in modulating river temperature (Lisi et al. 2015, Winfree et al. 2018).  
51 Despite conceptual agreement about hypothesized drivers of thermal sensitivity, substantial uncertainty persists  
52 regarding the relative importance of these covariates in controlling and predicting thermal sensitivity.

53 Empirical stream thermal sensitivity has been widely used to characterize historical stream temperature  
54 conditions and to predict how streams might respond to future climate warming (Mohseni et al. 2003, Mantua et al.  
55 2010). Generally, larger thermal sensitivities indicate that water temperatures are more likely to track changes in air  
56 temperature (Isaak et al. 2016, Mauger et al. 2017, Isaak et al. 2018b). However, there are concerns about using  
57 current-day thermal sensitivities to predict future stream temperatures, as it can be difficult to derive insights about  
58 river response to perturbations from statistical models that rely on historical relationships that may not extrapolate  
59 well to future conditions. For example, past studies have found that using empirical relationships for extrapolating to  
60 future climate scenarios without accounting for underlying processes such as snowmelt, groundwater, and annual  
61 hysteresis may provide inaccurate predictions of future stream temperatures (Leach and Moore 2019, Steel et al. 2019).

62 Under changing climatic conditions, the interrelations between air temperature and other processes controlling stream  
63 temperature may not remain stable (Arismendi et al. 2014). Additionally, stream networks can exhibit patchy thermal  
64 conditions due to spatially heterogeneous landscape attributes such as riparian shading, valley form and aspect, and  
65 geology (Bogan et al. 2003, Benyahya et al. 2010). Large-scale models that do not incorporate fine-scale variation in  
66 thermal sensitivity may not accurately predict thermal habitat at ecologically relevant scales. Despite these  
67 shortcomings, thermal sensitivity remains a commonly used and straightforward tool that allows for comparison  
68 between locations within rivers and has the potential to guide management.

69         There is a need to better understand how thermal sensitivities evolve throughout the year and along river  
70 networks and to develop a clearer understanding of the relationships between derived model coefficients and important  
71 watershed processes. Furthermore, thermal sensitivity itself can vary across time and space, rendering stationary  
72 values insufficient to describe variability in this parameter. A clearer vision of how thermal sensitivities vary would  
73 allow natural resource managers to understand what a single snapshot in time or space represents and could provide  
74 insight into how river thermal sensitivity may evolve under nonstationary air temperature and precipitation regimes.  
75 Groups of streams (clusters) that share similar patterns of thermal sensitivity will likely also share similar risk profiles.  
76 Identification of stream clusters could help managers tailor investment in streams according to watershed-specific  
77 influences (Mayer 2012). This study aims to answer three questions across two Pacific Northwest river basins: **1)**  
78 **What is the spatial and temporal distribution of commonly used thermal sensitivity metrics across each basin? 2)** **What**  
79 **are the representative thermal sensitivity regimes , how do they cluster on the landscape, and how do these clusters**  
80 **differ from clusters based on air and water temperature individually? and 3)** **What are the landscape or climate factors**  
81 **that best predict thermal sensitivity cluster membership? Finally, we consider the statistical functionality of these**  
82 **methods on river networks.**

## 83 **2 Methods**

### 84 **2.1 Study Area**

85 The Snoqualmie River begins as three distinct forks in the Mt. Baker Snoqualmie National Forest and drains a 1,813  
86 km<sup>2</sup> watershed on the west side of the Cascade Range, Washington (Figure 1). The three forks originate in forested  
87 public land before converging and flowing through a mix of agricultural, residential, and commercial land use. On  
88 one major tributary, the Tolt River, a dam and a large reservoir provide drinking water for the City of Seattle (Figure

89 S4). The Wenatchee River drains 3,440 km<sup>2</sup> of the eastern Cascades before flowing into the Columbia River (Figure  
90 S5). Although land use is similar to the Snoqualmie basin, wherein the headwaters originate in forested public lands  
91 before flowing through a mix of agricultural, residential, and commercial land use, forest density is generally lower  
92 in the eastern Cascades.

93 Both the Snoqualmie and Wenatchee basins have a Mediterranean climate with dry summers and wet, mild  
94 winters influenced by proximity to the Pacific Ocean. The climate on the east side of the Cascades is drier than that  
95 of the west side; the average annual precipitation is 1874 mm (939 mm) and the average annual temperature is 5.7°C  
96 (5.3°C) for the western (eastern) Cascades . However, the prevailing westerly winds, which cross the Cascades, create  
97 temperature and precipitation gradients that vary widely across the Wenatchee basin. In both basins, precipitation  
98 occurs predominately from October to March. The coldest month is typically January, whereas the warmest is July.  
99 Rivers have a mixed rain-snow hydrology with substantial winter rain and spring snowmelt, although the Wenatchee  
100 basin receives more winter precipitation as snow. Peak flow generally occurs during winter in the Snoqualmie River  
101 and spring in the Wenatchee River (Figure 2). Geology differs across the basins. Geology of the Snoqualmie basin is  
102 characterized by a deep glacial aquifer in the lowland portion of the watershed, whereas in the alpine area much of the  
103 ground surface is directly underlain by bedrock that lacks significant fracture systems (Turney et al. 1995, Bethel  
104 2004). In contrast, the Wenatchee basin's geology consists of both an aquifer within the sedimentary bedrock of the  
105 central and lowland areas and an overlying unconsolidated alluvial and outwash aquifer located primarily in river  
106 valley bottoms (Montgomery Water Group 2003). The Snoqualmie and Wenatchee basins both have reaches where  
107 water temperature exceeds regulatory thresholds established for salmonids that are protected by the U.S. Endangered  
108 Species Act (ESA). Both basins support ESA-listed Chinook Salmon (*Oncorhynchus tshawytscha*) and Steelhead  
109 Trout (*Oncorhynchus mykiss*) and the Wenatchee basin additionally supports populations of Bull Trout (*Salvelinus*  
110 *confluentus*) and Sockeye Salmon (*Oncorhynchus nerka*).

111 Water temperature loggers ( $N_{\text{Snoqualmie}}=42$ ,  $N_{\text{Wenatchee}}=31$ ) were installed throughout the mainstems, on major  
112 tributaries and on a selection of minor tributaries for both the Snoqualmie and Wenatchee rivers (Figure 1). Practical  
113 limitations forced sites to be publicly accessible, or on private property with landowner permission, and within 1 km  
114 of a road. For this study, water temperature was recorded using HOBO TidbiT v2 (UTBI-001) loggers every hour  
115 from October 1, 2014 through September 30, 2021 in both basins. We hereafter use North American hydrologic years  
116 (1 October – 30 September) instead of calendar years with the year of summer data as the year of reference. Air

117 temperature data was recorded using HOBO Pendant (UA-002-64) loggers every hour at all water temperature  
118 monitoring sites. Air temperature was logged for subset of 11 (6) sites in the Snoqualmie (Wenatchee) basin beginning  
119 October 1, 2014, and for all sites beginning October 1, 2016 (October 1, 2018). Air loggers were placed on trees along  
120 the stream bank, as close to the stream temperature loggers as possible. The air temperature loggers were secured at  
121 approximately breast height on the north side of the trees. Solar shields were fashioned to house both water and air  
122 temperature loggers.

## 123 **2.2 Exploratory analysis of air-water correlation summary metrics**

124 We calculated two summary metrics to characterize the relationship between air temperature and water temperature.  
125 For each site, summary metrics were derived from linear regressions between mean daily values of air and water  
126 temperature. The slope of this relationship, the thermal sensitivity, indicates the average difference in water  
127 temperature when comparing time periods with a one-degree difference in air temperature. For example, a thermal  
128 sensitivity of 0.5 would indicate that, based on historical data, when air temperature at a site differs by 1°C, water  
129 temperature differs on average by 0.5°C (Leach and Moore 2019). The strength of this relationship ( $R^2$ ) is an indicator  
130 of how well water temperature can be approximated by air temperature and is calculated as the Pearson correlation  
131 value between air and water temperature. Summary metrics were calculated separately for each season. Seasons were  
132 defined as fall (October, November, December), winter (January, February, March), spring (April, May, June), and  
133 summer (July, August, September).

134 Watersheds for each site were delineated and covariates describing the watersheds were obtained from  
135 commonly available geostatistical products (Table 2). Covariates were divided into four broad categories: basin  
136 topography (watershed area, mean watershed elevation, average stream slope, and distance upstream), land use  
137 (percent watershed forest, riparian forest, and lake area), climate (average temperature, precipitation, and percent  
138 precipitation falling as snow), and hydrogeologic (baseflow index, hydraulic conductivity, and soil depth to bedrock).  
139 Temperature, precipitation, and percent precipitation as snow were obtained from DAYMET Daily Surface Weather  
140 data (Thornton et al. 2020) and all other landscape covariates were obtained from the Stream-Catchment (StreamCat)  
141 Database (Hill et al. 2016).

142 A large body of literature examines landscape-level drivers of air and water temperature correlations within  
143 rivers. Therefore, we first summarized hypothesized drivers of thermal sensitivity based on previous literature and  
144 their covarying landscape variables within our basins (Table 1A). We then conducted an exploratory analysis of the

145 relationship between landscape covariates and thermal sensitivity to better understand patterns in our data and set up  
146 future hypothesis testing. Due to the correlated nature of our dataset, no formal statistical tests were conducted. We  
147 plotted summer thermal sensitivity against hypothesized drivers, including mean watershed elevation (MWE),  
148 watershed slope, distance upstream, percent riparian forest cover, and substrate hydraulic conductivity. Loess curves  
149 were plotted to aid in data visualization, and correlation coefficients between thermal sensitivity and each landscape  
150 covariate were used to quantify the strength of the linear relationship.

151 We also explored the relationship between spring thermal sensitivity and snowmelt, defined as the change in  
152 Snow Water Equivalent (SWE) for a given season and denoted as  $\Delta\text{SWE}$ , and between summer thermal sensitivity  
153 and mean air temperature and total precipitation. Climatic variables were obtained from gridded DAYMET data  
154 products (Thornton, et al. 2020) and calculated for the upstream catchment of each monitoring station.

### 155 **2.3 Spatially weighted clustering of thermal sensitivity, water temperature, and air temperature**

156 To identify representative regimes of air-water temperature correlations, we employed a varying-coefficient linear  
157 model to obtain continuous, daily estimates of thermal sensitivity. We then defined a spatially weighted dissimilarity  
158 matrix for use in clustering, which quantifies the spatial correlation in thermal sensitivity time series while accounting  
159 for the directed river network structure. We used this spatially weighted dissimilarity matrix with agglomerative  
160 hierarchical clustering to identify groups of sites exhibiting similar patterns in thermal sensitivity over time and  
161 compared these clusters to those generated using only water or air temperature. Details of each step are provided in  
162 the following sections.

#### 163 **2.3.1 Varying coefficient linear model for air-water relationship**

164 To derive a continuous thermal sensitivity metric, we fit a time-varying coefficient model (TVCM) to air and water  
165 temperature data. The TVCM is an effective tool for exploring dynamic features of the sensitivity of water temperature  
166 with changes in air temperature and uses a parametric linear model but with time-varying coefficients (Li et al. 2014,  
167 2016). For a given site, we described the varying coefficient model for the air–water temperature relationship as:

$$168 \quad y_t = \beta_{0,t} + x_t \beta_{1,t} + \epsilon_t, t = 1, \dots, T \quad (1)$$

169 Where  $\beta_{0,t}$  and  $\beta_{1,t}$  are varying intercept and slope coefficients. To estimate the time-varying coefficients, we adopted  
170 an ordinary least squares kernel regression with the Nadaraya–Watson estimator, where we fit a set of weighted local  
171 regressions with an optimally chosen window size defined by the bandwidth,  $b$ , and the weights given by the kernel

172 function (Hoover 1998, Casas and Fernandez-Casal 2019). The kernel and its bandwidth control the level of smoothing  
173 by adjusting the weight that the neighbouring time points have on estimates at  $t$ . The bandwidth was set to 0.2 a priori  
174 to ensure consistency across time series. We used the Gaussian kernel that is of the form  $k(x) = \frac{1}{2} \pi e^{-\frac{x^2}{2}}$ . The varying  
175 intercept term represents the mean water temperature at time  $t$  and the varying slope term represents the local  
176 sensitivity of water temperature to changes in air temperature at time  $t$ . We used the R package tvReg (Casas and  
177 Fernandez-Casal 2021) for implementing the model.

178 We filtered resultant time series for site-years with  $> 218$  days (60% of the year) and gaps of  $\leq 7$  days,  
179 yielding 250 site-years from 73 sites across both the Snoqualmie and Wenatchee basins. To capture the typical range  
180 and timing of thermal sensitivity at each site, we created a single representative time series of thermal sensitivity at  
181 each site by calculating the mean daily thermal sensitivity for each day of the year across all years of filtered data. We  
182 use this average annual time series for subsequent clustering analyses. To ensure that using an average annual time  
183 series of thermal sensitivity was an appropriate choice given the structure of our data, we conducted a supplementary  
184 analysis to assess cluster sensitivity to interannual variability (Appendix A). Measured air and water temperature and  
185 modelled thermal sensitivities for each site can be visualized at the following link:  
186 [https://lmcgill.shinyapps.io/TimeVarying\\_AWC/](https://lmcgill.shinyapps.io/TimeVarying_AWC/).

### 187 2.3.2 Estimating a spatially weighted dissimilarity matrix

188 To quantify spatial correlation while accounting for the directed river network structure, we developed a dissimilarity  
189 measure for time series of thermal sensitivity, water temperature, and air temperature that incorporated spatial  
190 correlation between sites (Haggarty et al. 2015). The general form of the proposed dissimilarity measure between sites  
191  $x$  and  $y$  can be written as:

$$192 d_{xy}^c = d_{xy} \widehat{cov}(h_s) \quad (2)$$

193 where  $d_{xy}^c$  is the spatially weighted dissimilarity matrix,  $d_{xy}$  is the Canberra distance (Lance and Williams 1967), and  
194  $\widehat{cov}(h_s)$  is a valid stream distance-based covariance matrix.

195 To estimate  $\widehat{cov}(h_s)$ , we used the tail-down model that was introduced by Ver Hoef and Peterson (2010).  
196 Due to the complex structure of the tail-down model, it is necessary to model spatial correlation on a river network  
197 with a covariogram. We first estimated the covariance between time series at each site using a classic formula from  
198 Cressie (1993), which states that the estimated covariance between sites  $x$  and  $y$  is given by

199 
$$\widehat{cov}(x, y) = \sum_{t=1}^T \frac{\{x_t - \bar{x}\}\{y_t - \bar{y}\}}{T} \quad (3)$$

200 where  $x_t$  and  $y_t$  are the values of the variable (thermal sensitivity, water temperature, or air temperature) at sites  $x$  and  
 201  $y$  at time  $t$  and  $T$  is the total number of discrete times. This results in a single value which summarizes the covariance  
 202 between the time series at the two sites over the period of interest. We then plotted these point summaries of the  
 203 covariance between pairs of curves against lags (measured as stream distance) to obtain an empirical stream distance-  
 204 based covariogram. We fit an exponential covariance function to this empirical covariogram and evaluated the model  
 205 at relevant distances to obtain an estimated stream distance-based covariance matrix  $\widehat{cov}(h_s)$ . We used this new  
 206 covariance matrix to weight the Canberra distance matrix as shown in Equation 2. The final spatially weighted  
 207 dissimilarity matrix,  $d_{xy}^c$ , was then used in clustering analyses.

### 208 **2.3.3 Agglomerative hierarchical clustering**

209 We used agglomerative hierarchical clustering (AHC) to identify groups of sites where the patterns in thermal  
 210 sensitivity, water temperature, and air temperature were similar over time using the hclust function in R (R Core Team  
 211 2020). AHC is a common clustering method (Olden et al. 2012, Maheu et al. 2016, Savoy et al. 2019, Isaak et al.  
 212 2020) where each time series starts in its own cluster, and the hierarchy is built by repeatedly merging pairs of similar  
 213 clusters separated by the shortest distance (i.e., measured as the similarity between individual times series) until all  
 214 points are contained in a single cluster. To decide which clusters are merged in every iteration, AHC uses a dissimilarity  
 215 metric ( $d_{xy}^c$ , derived in Equation 2) and a linkage criterion. We used Ward’s minimum variance linkage method for  
 216 clustering, where the distance between two clusters is computed as the increase in the sum of squared differences after  
 217 combining two clusters into a single cluster. The shortest of these links (minimum increase in the sum of squared  
 218 differences) that remains at any step causes the fusion of the two clusters whose elements are involved.

219 A difficulty associated with cluster analysis is determining the most appropriate number of clusters given the  
 220 data because no a priori optimal number of clusters exists. Clusters resulting from alternative choices can be evaluated  
 221 through internal cluster validity indices (CVI); there are a variety of CVIs, most of which combine within cluster  
 222 cohesion (intra-cluster variance) or between cluster separation (inter-cluster variance) to compute a quality measure.  
 223 There is no universally best CVI (Arbelaitz et al. 2013), therefore we calculated a suite of five CVIs, including the  
 224 Silhouette, Gap, Davies–Bouldin, Calinski–Harabasz, and generalized Dunn indices, using the NbClust R package



225 (Charrad et al. 2014). A final number of clusters was determined by a majority rules approach based on the optimal  
226 number of clusters suggested by each index (Table S2).

227 To determine whether clusters assignment were stable, or preserved under a perturbed dataset similar to the  
228 original and therefore likely reflective of real differences, we conducted a bootstrapping approach where sites were  
229 sampled with replacement and then AHC was performed on the resampled data using the *fpc* R package (Hennig  
230 2020). For each bootstrapped cluster, we assessed the similarity between each new cluster and the most similar original  
231 cluster with the Jaccard index. The Jaccard coefficient ranges from 0 to 1. Clusters with a coefficient larger than 0.75  
232 were considered stable, clusters with a coefficient between 0.5 and 0.75 indicate that the cluster is measuring a pattern  
233 in the data but exact site assignment may be doubtful, and clusters with a mean Jaccard coefficient of less than 0.5  
234 were considered unstable and may not reflect a true pattern in the data (Maheu et al. 2016, Savoy et al. 2019). We  
235 repeated the bootstrapping procedure 10,000 times; the mean Jaccard coefficient for each cluster is reported in Table  
236 4.

#### 237 **2.3.4 Identification of environmental drivers in thermal sensitivity**

238 We used classification and regression trees (CART; Breiman et al. 1984) to investigate the relative importance of  
239 basin topography, land use, climate, and hydrogeologic attributes (Table 2) for predicting each site's membership to  
240 a thermal sensitivity cluster. CART is typically used to attempt to predict membership to clusters using environmental  
241 attributes, and it allows the modelling of nonlinear relationships among mixed variable types and facilitates the  
242 examination of intercorrelated variables in the final model (De'ath and Fabricius 2000, Olden et al. 2008). We took  
243 an exploratory approach to this analysis due to our relatively small sample size ( $N_{\text{Snoqualmie}} = 42$ ,  $N_{\text{Wenatchee}} = 31$ ), which  
244 limited our ability to conduct statistical tests. Therefore, we calculated variable relative importance, defined as the  
245 sum of squared improvements at all splits determined by the predictor. These values are scaled to sum to 100  
246 (rounded). To ensure no single site unduly impacted CART results (Krzywinski and Altman 2017), we conducted a  
247 supplementary leave-one-out-cross-validation analysis to ensure relative importance estimates were stable across  
248 different permutations of the data (Figure S7). We used the R package *rpart* (Therneau and Atkinson 2019) for  
249 implementing the CART model.

## 250 **3 Results**

### 251 **3.1 General patterns in temperature, precipitation, and thermal sensitivity**

252 This analysis included data from seven hydrologic years, each with differing temperature and precipitation patterns.  
253 Generally, the years spanned by our dataset were warmer than the historical average (1901-2000), with wetter than  
254 average winter and fall months and drier spring and summer months (Figure S1). For the western (eastern) Cascades,  
255 all years (2015-2021) have average annual temperatures higher than the long-term average of 8.6 °C (3 °C), although  
256 individual seasons were slightly cooler than average. The year 2015 stood out as a year with an exceptionally warm  
257 winter, low snowpack, and dry spring. Temperature and precipitation patterns in the western and eastern Cascades  
258 were generally similar, however, precipitation anomalies were typically smaller in the eastern Cascades due to the  
259 overall lower precipitation in this region (Figure 2; Figure S1).

260 Summary metrics describing air-water temperature relationships exhibited substantial variation across time  
261 (season and year) and space. Across all season-year combinations, thermal sensitivities ranged from 0.05 to 0.97  
262 (mean = 0.54) in the Snoqualmie basin and from 0.06 to 0.74 (mean = 0.42) in the Wenatchee basin (Table 3). Seasonal  
263 distributions of thermal sensitivities also differed. For example, fall thermal sensitivities in both basins were relatively  
264 homogeneous, with 90% of values falling between 0.47 and 0.70, whereas spring and summer thermal sensitivities  
265 exhibited a broader range of values, with 90% of values falling between 0.30 and 0.84 in spring and 0.25 and 0.78 in  
266 summer. Air temperature was generally a good predictor of water temperature, as evidenced by  $R^2$  values that ranged  
267 from 0.20 to 0.99 (mean = 0.88) in the Snoqualmie basin and from 0.08 to 0.98 (mean = 0.85) in the Wenatchee basin  
268 (Table 3).

269 Overall, weak and inconsistent patterns emerge in summer between thermal sensitivity and landscape and  
270 climate variables (Figure 3; Table 1B). For climate variables, only  $\Delta$ SWE appeared to have a relationship with thermal  
271 sensitivity (Figure 3). The relationship between  $\Delta$ SWE and thermal sensitivity was negative and non-linear, displaying  
272 a wedge-shaped pattern wherein large snowmelt events did not reduce thermal sensitivities below 0.25 (Figure 3). For  
273 landscape variables, correlation coefficients were overall small ( $|\rho| < 0.3$ ), indicating weak to non-existent linear  
274 relationships between landscape covariates and observed thermal sensitivity (Table 1B). A weakly negative  
275 relationship between thermal sensitivity and distance upstream was observed for both basins. Percent riparian forests  
276 and thermal sensitivity showed no relationship for either basin. The relationship between hydraulic conductivity and  
277 thermal sensitivity was weakly positive and parabolic in the Snoqualmie basin.

### 278 **3.2 Patterns of clustering for water temperatures, air temperatures, and thermal sensitivities**

279 Time-varying thermal sensitivities displayed periods of both high and low values within a season, which was not  
280 necessarily represented when looking only at seasonal summary metrics (Figure 4 and Figure 5). Thermal sensitivity  
281 varied alongside water and air temperature within the Snoqualmie and Wenatchee basins. Generally, thermal  
282 sensitivity rose sharply in late spring, was highest in late summer, declined slowly throughout the fall, and remained  
283 depressed through winter and early spring.

284 Spatially weighted AHC yielded four clusters for thermal sensitivity, with a cluster validity index (CVI)  
285 range of 2-4, and two clusters each for air (CVI range of 2-5) and water (CVI range of 2-4) temperature in the  
286 Snoqualmie basin, and five clusters for thermal sensitivity (CVI range 2-5) and two clusters each for air (CVI range  
287 of 2-3) and water (CVI range of 2-5) temperature in the Wenatchee basin (Figure 4; Figure 5; Table S2). For both  
288 basins, clusters of air and water temperature correspond closely with elevational gradients (Figure S4; Figure S5).  
289 Higher elevation sites exhibited generally lower magnitudes but similar patterns in air and water temperatures (Table  
290 4). For example, within both basins seasonal water temperatures were synchronized, with the cluster minimum and  
291 maximum water temperatures occurring within a day of each other (Table 4). In the Snoqualmie basin, air temperature  
292 clusters were stable, with a mean Jaccard index of 0.91 for high elevation sites (Cluster 2, n=11 sites) and 0.73 for  
293 low elevation sites (Cluster 1, n=31 sites). Water temperature clusters were slightly less stable, with a mean Jaccard  
294 index of 0.65 for high elevation sites (Cluster 2, n=17 sites) and 0.89 for low elevation sites (Cluster 1, n=25 sites).  
295 Air and water temperature clusters in the Wenatchee basin were more stable than the Snoqualmie clusters. In the  
296 Wenatchee basin, air temperature clusters had a mean Jaccard index of 0.85 for high elevation sites (Cluster 2, n=25  
297 sites) and 0.95 for low elevation sites (Cluster 1, n=6 sites), and water temperature clusters had a mean Jaccard index  
298 of 0.86 for high elevation sites (Cluster 2, n=23 sites) and 0.73 for low elevation sites (Cluster 1, n=8 sites).

299 Clustering patterns for thermal sensitivity were more complex and less stable than air and water temperature  
300 clusters, particularly for the Snoqualmie basin (Figure 4; Figure 5; Table 4). In the Snoqualmie basin, Cluster 1 (n=11  
301 sites) consisted primarily of low elevation tributaries that exhibited stable thermal sensitivities throughout the year,  
302 producing a cluster-average range of only 0.15 (Figure 4; Table 4). Cluster 2 was small (n=5 sites), and the distribution  
303 of sites within this cluster included three mainstem sites and two high elevation tributaries. Despite the large  
304 geographic distances separating sites, this cluster was highly stable with a mean Jaccard index of 0.88. Cluster 2 was  
305 characterized by a mean thermal sensitivity of 0.52 and the highest annual variability, with a cluster-average range of

306 0.45. Cluster 3 was large (n=15 sites) and contained sites located within the upper regions of the Snoqualmie River.  
307 Cluster 3 had the lowest mean thermal sensitivity (mean=0.40). Lastly, Cluster 4 (n=11 sites) exhibited the lowest  
308 stability of any cluster in the Snoqualmie basin, with a mean Jaccard index of 0.55. Sites in this cluster were mainly  
309 situated on the mainstem Snoqualmie and its major tributaries. This cluster was distinguished by the highest mean  
310 thermal sensitivity (mean=0.65). In the Wenatchee basin, all five thermal sensitivity clusters were relatively stable.  
311 Clusters 1 (n=7 sites), 4 (n=8 sites), and 5 (n=8 sites) demonstrated similar seasonal patterns in thermal sensitivities,  
312 with minimum values occurring in late Spring (water days 216, 207, 214) and maximum values occurring in late  
313 summer (water days 324, 331, 330). These clusters also showed moderate to high stability (mean Jaccard indices of  
314 0.79, 0.86, and 0.79). Cluster 3 (n=7 sites) exhibited the highest mean thermal sensitivity (mean=0.40) and  
315 encompassed primarily low elevation tributaries (Peshastin and Mission Creek; Figure S5). Cluster 2 was unique in  
316 that it consisted of a single site (Chumstick Creek) that was nearly always assigned to a unique cluster when included  
317 in the bootstrapping procedure. The thermal sensitivity for this site was low (mean=0.29) and virtually flat throughout  
318 the year (range = 0.07).

319 CART analysis indicated that basin topography and hydrogeologic attributes were the principal  
320 discriminators of thermal sensitivity clusters. The top predictors of cluster membership (i.e., predictors with a greater  
321 than 10% increase in mean standard error if removed from the model) were MWE and baseflow index in the  
322 Wenatchee basin and watershed slope, MWE, and soil depth in the Snoqualmie basin (Figure 6). Variable importance  
323 distributions differed between the Wenatchee and Snoqualmie basins, although in both basins several covariates had  
324 similar relative importance values. Covariate distributions also varied across clusters within a basin. In the Snoqualmie  
325 basin, Cluster 1 sites were generally below a MWE of 600 meters, whereas Cluster 3 sites were generally mid-sized  
326 and high elevation with a low baseflow index. In the Wenatchee basin, Cluster 1, 4, and 5 sites were predominately  
327 located at high elevations with steep slopes. Cluster 4 sites exhibited a large proportion of precipitation falling as rain.  
328 Sites in Clusters 2 and 3 were generally low elevation sites with a high baseflow index and soil depth.

#### 329 **4 Discussion**

330 Thermal sensitivity varies throughout the year and reflects hydrologic conditions at a given time and place within a  
331 watershed; therefore, it should not be conceptualized as a static value. Although summary metrics of thermal  
332 sensitivity, such as average values over the summer, can still prove useful and informative, it is essential to

333 acknowledge the non-stationarity of the relationship between air and water temperature to obtain an accurate  
334 understanding of how river temperature responds to changing conditions. We find that underlying geology and climate  
335 are important controls on thermal sensitivity across two Pacific Northwest river basins, and thermal sensitivities reflect  
336 aspects of river dynamics not redundant with water and air temperature. Overall, this study provides a framework for  
337 using thermal sensitivity regimes to improve understanding of factors contributing to stream temperatures and will  
338 enable managers to target mitigation and adaptation activities to work best with local conditions within a watershed.

#### 339 **4.1 Patterns of thermal sensitivity clustering**

340 Our analysis of stream air and water temperatures supports the presence of distinct thermal sensitivity regimes,  
341 providing an organizing framework for river research and management by identifying sites with similarities across the  
342 network. We found that thermal sensitivity regimes reflected non-redundant aspects of river dynamics relative to air  
343 and water temperature alone. Air temperature and water temperature clusters closely corresponded to one another and  
344 were almost entirely determined by elevation of the temperature loggers, whereas thermal sensitivity clusters showed  
345 more variability in annual patterns and were intermixed spatially (Figure 4; Figure 5). Previous studies within the  
346 Pacific Northwest found that, generally, colder streams are less sensitive to air temperature fluctuations than warmer  
347 streams (Luce et al. 2014, Kelleher et al. 2021). Air and water clustering results are consistent with previous studies  
348 that observed broad temporal correspondence of air and river temperature dynamics with differing magnitudes of  
349 response (Bower et al. 2004, Chu et al. 2010, Garner et al. 2014, Isaak et al. 2018a). More locally, Isaak et al. (2020)  
350 found that across western rivers, much of the information in stream temperature records could be summarized by a  
351 relatively limited number of distinct regime components primarily driven by differences in elevation and latitude.

352 Viewing thermal sensitivity as a continuous parameter adds novel insights to our understanding of river basin  
353 functioning. Studies have highlighted the importance of annual shifts in the processes that drive heat budgets as well  
354 as the non-stationarity of the resulting statistical relationships (Arismendi et al. 2014, Boyer et al. 2021). Our clustering  
355 analysis overcomes these issues by using a varying coefficient model that treats thermal sensitivity as a continuous  
356 function through time, rather than a series of discrete summary metrics, and allows clustering based on the entirety of  
357 average annual patterns. The observed complexity in thermal sensitivity response hints at the diversity of physical  
358 processes controlling stream temperature response and the large, clear shifts in thermal sensitivity magnitude across  
359 the year calls into question the common practice of summarizing a river's sensitivity as a static value. The ability to  
360 directly observe shifts in the air-water temperature relationships also opens the possibility of using thermal sensitivity

361 as a diagnostic tool to examine gradual changes in the importance of drivers of water temperature, such as dynamic  
362 changes in riparian shading or snowmelt.

#### 363 **4.2 Climate controls on thermal sensitivity**

364 Seasonal variability of thermal sensitivity metrics was evident for our basins. Within both the Snoqualmie and  
365 Wenatchee basins, winter thermal sensitivities were low and varied strongly with MWE (Figure 1). Observed low  
366 thermal sensitivities in winter were likely due to the non-linear relationship between air and stream temperature at  
367 cold temperatures when air temperatures can dip below the water temperature-freezing limit (Mohseni et al. 1998,  
368 1999). Air temperature covaries strongly with elevation in Pacific Northwest basins, and sites that are high in the  
369 watershed will experience a greater number of sub-freezing days, and therefore greater decoupling between air and  
370 water temperatures. Fall thermal sensitivities were relatively homogeneous whereas spring and summer thermal  
371 sensitivities exhibited a broader range of values. We expect thermal sensitivities to be similar during periods of heavy  
372 precipitation, when water sources with thermal characteristics distinct from air temperature, such as groundwater and  
373 snowmelt, contribute relatively less flow. The greater variability of responses in spring and summer indicates that the  
374 relative magnitude of energy exchange processes controlling river temperatures are more diverse than in fall or winter  
375 (Hrachowitz et al. 2010).

376 Snowmelt likely contributed to observed differences in thermal sensitivity across sites in spring and early  
377 summer. For summary metrics, the relationship between snowmelt and spring thermal sensitivity formed a wedge-  
378 shaped pattern, wherein sites with limited snowmelt displayed both high and low thermal sensitivity, but sites with  
379 extensive snowmelt always display low thermal sensitivity (Figure 3). For the clustering analysis, although the  
380 proportion of precipitation falling as snow showed limited variable importance, MWE and slope covaried closely with  
381 snow accumulation and were among the most important predictors of cluster membership, perhaps masking a  
382 statistical signal of snowfall (Figure 6). In both the Snoqualmie and Wenatchee basins, clusters with higher elevation,  
383 steeper slope, and greater snowmelt within the catchment had thermal regimes that were less sensitive to changes in  
384 air temperature during spring and early summer. Importantly, snowmelt buffering, the process wherein snowmelt-  
385 influenced streams have lower thermal sensitivity due to a direct input of cold water and a corresponding increase in  
386 flow rates and water depths (van Vliet et al. 2011, Siegel et al. 2022), diminishes throughout the summer. By late  
387 summer, high elevation, snowmelt influenced sites were often more sensitive to air temperatures than their low  
388 elevation counterparts (Figure 4; Figure 5). Sites within Cluster 4 in the Wenatchee basin were an exception to this

389 pattern and maintained summer thermal sensitivities that were substantially depressed relative to adjacent locations  
390 (e.g., Clusters 1 and 5). This is likely due to continuous summer snowmelt inputs within these catchments, and points  
391 to the importance of high elevation, late-summer snowpack melt as a significant source of summer baseflow and  
392 control on water temperatures during the months of greatest heating within these watersheds.

393 Numerous studies have examined the buffering impact of snowmelt on water temperature due to advective  
394 flux from cooler meltwater entering the river. Studies in Alaskan rivers found a linear, negative relationship between  
395 summer thermal sensitivity and snowmelt (Lisi et al. 2015, Cline et al. 2020) and a recent study in the Snoqualmie  
396 basin found that snowmelt can reduce basin-wide peak summer temperatures, particularly at high elevation tributaries,  
397 and the thermal impacts of melt water can persist through the summer (Yan et al. 2021). Our results suggest that  
398 snowpack offers substantial buffering to changes in air temperature across mountain river basins, but that the largest  
399 impacts are localized across space and time. Climate change is expected to shift snowmelt earlier and reduce snow  
400 water resources (Barnett et al. 2005, Musselman et al. 2021). The loss of snow may result in warming in snow-  
401 influenced systems and the subsequent homogenization of thermal conditions across basins (Winfrey et al. 2018).  
402 Homogenization of thermal conditions likely leads to important changes in ecological functions and ecosystem  
403 services supported by lost thermal heterogeneity, such as a loss of cold-water patches for Pacific salmon (Brennan et  
404 al. 2019).

#### 405 **4.3 Hydrogeologic controls on thermal sensitivity**

406 Hydrogeologic characteristics shaped the relationship between air and water temperatures across the Wenatchee and  
407 Snoqualmie basins. The inclusion of baseflow index, hydraulic conductivity, and soil depth in determining cluster  
408 membership (Figure 6) implies the importance, and detectability, of groundwater as a key mediator of thermal  
409 sensitivity regimes in Pacific Northwest basins. Clusters with high baseflow index, hydraulic conductivity, and soil  
410 depth values generally had lower summer and less variable thermal sensitivities (Figure 4; Figure 5; Figure 6),  
411 implying greater groundwater influence (Kelleher et al. 2012). Interestingly, despite the clear importance of  
412 hydrogeologic metrics in the clustering analysis, results from summary metric exploratory analysis were mixed and,  
413 in the Snoqualmie basin, did not align with expectations of a negative relationship between thermal sensitivity and  
414 groundwater influence (Table 1B). Although it is possible to infer broad patterns in surface-groundwater connectivity  
415 using datasets of interpolated geologic properties (i.e., hydraulic conductivity, soil depth) or water source (i.e.,  
416 baseflow index), individual hydrogeologic metrics often have substantial uncertainty, do not covary perfectly, and

417 may be particularly unconstrained for mountain headwater streams (Wolock et al. 2004, Patton et al. 2018, Briggs et  
418 al. 2022). Additionally, the influence of these processes can be localized and variable across space (Johnson et al.  
419 2017) and substantially impacted by human modification. The ability to use thermal sensitivity as an empirical  
420 measure of groundwater influence, therefore, shows great promise for understanding catchment processes and  
421 informing management and restoration actions at ecologically relevant scales (Snyder et al. 2015). Although our  
422 approach moves us closer to a mechanistic understanding of the relationship between thermal sensitivity and  
423 groundwater, mixed results from our analyses emphasize the need for additional targeted studies.

424         An investigation of the underlying geology across the Snoqualmie and Wenatchee basins supports our  
425 conclusion that low thermal sensitivities are indicative of groundwater inputs. The lowland portion of the Snoqualmie  
426 watershed contains a deep, permeable, productive glacial aquifer that is presumed to be the source of summer baseflow  
427 to much of the river (Bethel 2004, McGill et al. 2021, Turney et al. 1995). Glacial and interglacial deposits in the  
428 valley contain several geohydrologic units with differing aquifer potential (Bethel 2004); however, most deposits can  
429 form small but useable aquifers that could be helping to sustain baseflow in summer months (Turney et al. 1995,  
430 Soulsby et al. 2004, Blumstock et al. 2015). Soil depth, hydraulic conductivity, and baseflow index were  
431 correspondingly high in streams from Clusters 1 and 4 that overlay the lower portion of the watershed (Figure 6).  
432 Thermal sensitivities reflected this pattern, wherein generally sites draining low elevation tributaries (Cluster 1) had  
433 relatively constant thermal sensitivities throughout the year (Figure 4). Conversely, the upper portion of the  
434 Snoqualmie basin is covered by thin soil over impermeable bedrock lacking extensive fracture networks, meaning that  
435 rain and snowmelt are not retained in the mountains but are rapidly transmitted to the stream system (Debose and  
436 Klungland 1964, Nelson 1971, Goldin 1973, 1992). Sites with catchments predominantly within this upland area  
437 tended to belong to Clusters 2 and 3 and displayed high summer thermal sensitivities, perhaps indicating limited  
438 groundwater buffering.

439         In the Wenatchee basin, two major aquifers exist: an aquifer within the sedimentary bedrock of the central  
440 and lowland areas and an overlying unconsolidated alluvial and outwash aquifer located primarily in river valley  
441 bottoms across the basin (Montgomery Water Group 2003). The bedrock aquifer consists of sandstones and shales,  
442 which tend to have moderately low permeability. Folding and faulting have caused the shale to break up or fracture  
443 and groundwater moves preferentially within these zones of higher secondary permeability. The alluvial and outwash  
444 aquifers, on the other hand, exhibit relatively high permeability where groundwater can move easily and are considered



445 the primary groundwater source (Wildrick 1979, Montgomery Water Group 2003). Cluster 2 in the Wenatchee basin,  
446 consisting of a single site located at the mouth of Chumstick Creek (Figure S5), stands out for having a unique, nearly  
447 flat thermal sensitivity compared to patterns at other sites (Figure 5). Covariate distributions for the clustering results  
448 showed that Chumstick Creek has a relatively high hydraulic conductivity and baseflow index (Figure 6; Figure S8).  
449 A transition from low to high permeability glacial material occurs near the mouth of Chumstick Creek (Montgomery  
450 Water Group 2003), and it is possible that substantial groundwater discharge occurs near this discontinuity (Neff et  
451 al. 2019). Similarly, sites within Cluster 3 showed low variability in thermal sensitivity and had high soil depth and  
452 baseflow index values. Streams within this cluster are situated on top of predominantly sandstone bedrock (Frizzell  
453 1979, Gendaszek et al. 2014).

454 Overall, the importance of groundwater is consistent with previous studies, which find that thermal sensitivity  
455 decreased with increasing groundwater contribution (O'Driscoll and DeWalle 2006, Chang and Psaris 2013, Beaufort  
456 et al. 2020, Georges et al. 2021). The degree to which groundwater decouples trends in stream and air temperature  
457 depends on stream volume, the rate of groundwater inflow, and the depth of groundwater source. Although not  
458 examined in this study, aquifer source and groundwater depth likely influence thermal sensitivity estimates, with  
459 runoff sourced from deep groundwater being less variable and less sensitive in comparison to groundwater sourced  
460 from shallow sub-surface flows (Tague et al. 2007, Johnson et al. 2021, Hare et al. 2021). Shallow groundwater  
461 temperatures are already responding to climate change (Menberg et al. 2014). As warming continues, the summer  
462 cooling capacity of groundwater may be reduced, limiting the availability of cold-water refugia patches sourced by  
463 groundwater (Brewer 2013, Briggs et al. 2013).

#### 464 **4.4 Landscape controls on thermal sensitivity**

465 Variable relationships between thermal sensitivities and landscape covariates highlight complexities in stream thermal  
466 regimes. For example, mean channel slope was an important predictor of cluster membership for both the Snoqualmie  
467 and Wenatchee basins but showed a weak-to-non-existent relationship with summer thermal sensitivity summary  
468 metrics. Steeper channel slopes and greater stream velocities limit warming in streams by decreasing the time for  
469 equilibration with local heating conditions (Donato 2002, Webb et al. 2008, Isaak et al. 2012) and topographic shading  
470 associated with steep watersheds can suppresses stream temperature by reducing exposure to solar radiation (Webb  
471 and Zhang 1997). In the Wenatchee basin, the Cluster 3 site, Chumstick Creek, drains a steep canyon. This may  
472 contribute to observed low, stable thermal sensitivities throughout the year. Additionally, watershed size and distance

473 upstream covary closely and displayed relatively consistent relationships with summer thermal sensitivity summary  
474 metrics despite ranking moderately in variable importance. We expected thermal sensitivity to increase with river size;  
475 groundwater influence should be more visible on smaller streams because the volume of water is small and the travel  
476 time of the water from the source is short and not sufficient to equilibrate water temperature with the atmosphere  
477 (Mohseni and Stefan 1999, Tague et al. 2007, Beaufort et al. 2016). Reduced sensitivity of headwater streams to air  
478 temperature was observed in the Aberdeenshire Dee, Scotland (Hrachowitz et al. 2010), and River Danube, Austria  
479 (Webb and Nobilis 2007), and small Pennsylvanian streams were shown to be less sensitive to changes in air  
480 temperature than larger streams (Kelleher et al. 2012). However, Hilderbrand et al. (2014) found no relationship  
481 between thermal sensitivity and watershed size in Maryland streams.

482 We expected landscape covariates to be important predictors of thermal sensitivity regimes, however, these  
483 covariates were of limited importance and showed no relationship with summary metrics (Table 1B; Figure 6). Several  
484 factors may account for this. Inherent covariation in river basins can hinder statistical efforts to identify mechanistic  
485 links between landscape gradients and features of aquatic ecosystems (Lucero et al. 2011); land cover characteristics  
486 may have a small impact that went undetected due to noisy observations or limited variability within our study region.  
487 It is also possible that land cover metrics may not adequately describe the intended process. For example, the relative  
488 unimportance of riparian shading may be due in part to our metric of shade, which was limited to riparian forest cover  
489 and ignored topographic shading and vegetation height. Lastly, human modifications to the river that are not captured  
490 by land cover statistics, such as channelization or the presence of dams and reservoirs, may alter thermal sensitivity  
491 and obscure natural gradients. For example, areas of the river that are degraded and subsequently disconnected from  
492 their floodplain may have artificially high thermal sensitivities, and the release of water from dams and reservoirs has  
493 the potential to either warm or cool downstream temperatures, depending on dynamics of where and how impounded  
494 water is released (Ahmad et al. 2021, Cheng et al. 2022). Future research could include covariates sinuosity or variance  
495 of thalweg depth to better capture these effects. Untangling exact controls will require additional research.

#### 496 **4.5 Assessment of statistical approach**

497 Collecting data on dynamic stream networks over time has inherent challenges that lead to relatively low sample sizes  
498 and missing data as well as complex correlation structures across space and time. Our statistical approach was  
499 designed to manage these challenges, enabling exploration of several hypotheses. These data, collected at a relatively

500 large number of sites in a parallel structure across two basins allow an assessment of how sensitive the statistical  
501 approach may be to these constraints.

502         The time series of both air and water temperature used in this analysis have periods of missing values that  
503 span weeks to months. Classical clustering techniques require complete datasets, limiting analyses to time series  
504 without gaps. To overcome this issue, we calculated a single representative time series at each site that captures the  
505 typical range and timing of thermal sensitivity. Alternative options for dealing with missing values include removing  
506 data points that do not cover the target time period or imputing missing values by means of statistical procedures or  
507 summary metrics (e.g., Savoy et al. 2019, Beaufort et al. 2020). However, we chose not to use these approaches in our  
508 study due to the long and inconsistent periods of missing values across sites. We acknowledge that interannual  
509 variability in precipitation and temperature impacts river thermal sensitivity, and average time series calculated from  
510 differing years may exhibit differences in shape and timing for reasons outside of inherent characteristics (Appendix  
511 A). Future studies could use novel clustering methods capable of dealing with sparse datasets, which would provide  
512 more detailed information on clusters generated from time periods with robust values versus data scarcity (Carro-  
513 Calvo et al. 2021). Alternatively, recent advances in space-time imputation for river basins may prove a fruitful  
514 direction (Li et al. 2017).

515         Our calculation of time-varying thermal sensitivities also necessitated decisions regarding what features of the  
516 time series to preserve. Selection of the bandwidth parameter and kernel function for the time varying model will  
517 impact estimation of thermal sensitivity and intercept. Generally, with larger bandwidth estimates or averaging periods  
518 (e.g., daily, weekly, monthly), intercept estimates increase and thermal sensitivity estimates decrease. Decisions of  
519 this nature should be approached carefully and with a clear question in mind. For this study, we were interested in  
520 seasonal to annual patterns in thermal sensitivity, and thus chose a bandwidth of 0.2, resulting in a smooth seasonal  
521 time series. Previous studies have also used regression splines to estimate the time varying relationship between air  
522 and water temperatures (Haggarty et al. 2015). This approach smooths data and can account for missing data but may  
523 not preserve small-scale features of interest. We chose to use absolute values of our thermal sensitivity time series, as  
524 we cared about differences in mean thermal sensitivity as well as correlated variability. Future work could normalize  
525 thermal sensitivity time series first to examine only patterns.

526         While general patterns could be detected through our analysis, the details were sensitive to exactly which  
527 sites were sampled and included in the analysis. In dynamic river systems with high spatial heterogeneity and inherent

528 difficulties with accessing certain areas of the network, this is always likely to be true. Our approach of averaging  
529 across years and clustering across sites appears to manage these realities well and provide general guidance on the  
530 river networks sampled. For example, cross validation results for CART modelling suggest that certain variables were  
531 consistently identified as more influential for cluster prediction and that results were relatively robust to the inclusion  
532 of individual data points (Figure S7). Strengthening the assessment of underlying drivers and controls to provide  
533 guidance for unsampled river networks will require that similar data sets are collected across more and more river  
534 networks. Data can then be assembled and analysed to provide more general conclusions about hydrogeologic, land  
535 use, and climatic controls of river thermal regimes.

#### 536 **4.6 Implications for management and future directions**

537 Classifying rivers based on thermal sensitivity could be a powerful tool when planning for global change. Our results  
538 show that annual patterns in thermal sensitivity are diverse and mediated by underlying geology and climate across  
539 two Pacific Northwest river basins. Climate change is decreasing snowpack in the region, resulting in earlier runoff  
540 and extended summer baseflow (Elsner et al. 2010, Wu et al. 2012), and may decrease groundwater discharge  
541 depending on sources and timing of recharge (Brooks et al. 2012, McGill et al. 2021). For many of our study sites,  
542 thermal sensitivities were highest in late summer during the hottest, lowest flow portion of the year. Previous studies  
543 have found that the impact of fluctuations in discharge generally increases during dry, warm periods, when rivers have  
544 a lower thermal capacity and are more sensitive to atmospheric warming (van Vliet et al. 2013). High thermal  
545 sensitivity in late summer and in high elevation streams, which are typically thought to be climate refuges, is therefore  
546 troubling for the conservation of native coldwater species such as Pacific salmon (Mantua et al. 2010; Isaak et al.  
547 2016). Climate change will likely decrease juvenile rearing and spawning habitat quantity and quality, although it is  
548 important to note that streams with high thermal sensitivity may still provide adequate habitat in select portions of the  
549 year if stress-related thresholds are not exceeded (Armstrong et al. 2021).

550 Examining thermal sensitivity regimes improves understanding of factors contributing to stream  
551 temperatures and may enable managers to target mitigation and adaptation activities to work best with local conditions,  
552 thus maximizing benefits given limited resources. For example, given the importance of subsurface geology within  
553 the Wenatchee and Snoqualmie basins, targeted actions to restore floodplain functions that recharge aquifers through  
554 actions such as placing engineered logjams or reintroducing beavers could be prioritized (Abbe and Brooks 2013,  
555 Pollock et al. 2014, Jordan and Fairfax 2022). Additionally, identification of particularly insensitive portions of the

556 river could help to better constrain areas where coldwater patches exist that may be used as refuges for coldwater fish  
557 (Snyder et al. 2020). This process-based approach will be particularly important as non-stationary relationships caused  
558 by climate change make it unreliable to use past regressions built under historical climate conditions (Boyer et al.  
559 2021). Furthermore, as longer, more spatially extensive air and water temperature time series become available (Isaak  
560 et al. 2017), we can begin to ask questions about 1) the spatial extent of different thermal sensitivity regimes, 2) how  
561 interannual variability shifts with climate conditions and geographic context, and 3) detect changes in the external  
562 drivers of thermal sensitivities. Such insights will improve our understanding of river ecosystems while offering a  
563 suite of new tools for monitoring the impact of management decisions and climate change.

#### 564 **Acknowledgements**

565 We thank Amy Marsha, Roxana Rautu, Akida Ferguson, Shannon Claeson and the many volunteers for help collecting  
566 air and water temperature data, and Gordon Holtgrieve, Mark Scheuerell, and Christopher Jordan for suggestions that  
567 improved the manuscript. This material is based upon work supported by the National Science Foundation Graduate  
568 Research Fellowship under Grant No. DGE-1762114. Any opinion, findings, and conclusions or recommendations  
569 expressed in this material are those of the authors and do not necessarily reflect the views of the National Science  
570 Foundation.

#### 571 **Author Contributions, Data Availability, and Competing Interests**

572 All authors conceptualized the study and retrieved the data. LMM analyzed the data and prepared the manuscript with  
573 the assistance of EAS and AHF. The data that supports the findings of this study are available at  
574 <https://github.com/lmcgill/AirWaterCorr/tree/master/data> and can be visualized at  
575 [https://lmcgill.shinyapps.io/TimeVarying\\_AWC/](https://lmcgill.shinyapps.io/TimeVarying_AWC/). The authors have no competing interests to declare.

576 **References**

- 577 Abbe, T., and A. Brooks. 2013. Geomorphic, Engineering, and Ecological Considerations when Using Wood in River  
578 Restoration. Pages 419–451 in A. Simon, S. J. Bennett, and J. M. Castro, editors. Geophysical Monograph  
579 Series. American Geophysical Union, Washington, D. C.
- 580 Ahmad, S. K., F. Hossain, G. W. Holtgrieve, T. Pavelsky, and S. Galelli. 2021. Predicting the Likely Thermal Impact  
581 of Current and Future Dams Around the World. *Earth's Future* 9.
- 582 Arbelaitz, O., I. Gurrutxaga, J. Muguerza, J. M. Pérez, and I. Perona. 2013. An extensive comparative study of cluster  
583 validity indices. *Pattern Recognition* 46:243–256.
- 584 Arismendi, I., M. Safeeq, J. B. Dunham, and S. L. Johnson. 2014. Can air temperature be used to project influences  
585 of climate change on stream temperature? *Environmental Research Letters* 9:084015.
- 586 Armstrong, J. B., A. H. Fullerton, C. E. Jordan, J. L. Ebersole, J. R. Bellmore, I. Arismendi, B. E. Penaluna, and G.  
587 H. Reeves. 2021. The importance of warm habitat to the growth regime of cold-water fishes. *Nature Climate  
588 Change* 11:354–361.
- 589 Barnett, T. P., J. C. Adam, and D. P. Lettenmaier. 2005. Potential impacts of a warming climate on water availability  
590 in snow-dominated regions. *Nature* 438:303–309.
- 591 Beaufort, A., F. Moatar, F. Curie, A. Ducharne, V. Bustillo, and D. Thiéry. 2016. River Temperature Modelling by  
592 Strahler Order at the Regional Scale in the Loire River Basin, France: River Temperature Modelling by  
593 Strahler Order. *River Research and Applications* 32:597–609.
- 594 Beaufort, A., F. Moatar, E. Sauquet, P. Loicq, and D. M. Hannah. 2020. Influence of landscape and hydrological  
595 factors on stream–air temperature relationships at regional scale. *Hydrological Processes* 34:583–597.
- 596 Benyahya, L., D. Caissie, N. El-Jabi, and M. G. Satish. 2010. Comparison of microclimate vs. remote meteorological  
597 data and results applied to a water temperature model (Miramichi River, Canada). *Journal of Hydrology*  
598 380:247–259.
- 599 Bethel, J. 2004. An overview of the geology and geomorphology of the Snoqualmie River watershed. King County  
600 Water and Land Resources Division, Snoqualmie Watershed Team.
- 601 Blumstock, M., D. Tetzlaff, I. A. Malcolm, G. Nuetzmann, and C. Soulsby. 2015. Baseflow dynamics: Multi-tracer  
602 surveys to assess variable groundwater contributions to montane streams under low flows. *Journal of  
603 Hydrology* 527:1021–1033.

604 Bogan, T., O. Mohseni, and H. G. Stefan. 2003. Stream temperature-equilibrium temperature relationship. *Water*  
605 *Resources Research* 39.

606 Bower, D., D. M. Hannah, and G. R. McGregor. 2004. Techniques for assessing the climatic sensitivity of river flow  
607 regimes. *Hydrological Processes* 18:2515–2543.

608 Boyer, C., A. St-Hilaire, and N. E. Bergeron. 2021. Defining river thermal sensitivity as a function of climate. *River*  
609 *Research and Applications* 37:1548–1561.

610 Breiman, L., J. H. Friedman, R. A. Olshen, and C. J. Stone. 1984. *Classification And Regression Trees*. First edition.  
611 Routledge.

612 Brennan, S. R., D. E. Schindler, T. J. Cline, T. E. Walsworth, G. Buck, and D. P. Fernandez. 2019. Shifting habitat  
613 mosaics and fish production across river basins. *Science* 364:783–786.

614 Brewer, S. K. 2013. GROUNDWATER INFLUENCES ON THE DISTRIBUTION AND ABUNDANCE OF  
615 RIVERINE SMALLMOUTH BASS, *MICROPTERUS DOLOMIEU* , IN PASTURE LANDSCAPES OF  
616 THE MIDWESTERN USA. *River Research and Applications* 29:269–278.

617 Briggs, M. A., P. Goodling, Z. C. Johnson, K. M. Rogers, N. P. Hitt, J. B. Fair, and C. D. Snyder. 2022. Bedrock depth  
618 influences spatial patterns of summer baseflow, temperature, and flow disconnection for mountainous  
619 headwater streams. preprint, *Catchment hydrology/Instruments and observation techniques*.

620 Briggs, M. A., Z. C. Johnson, C. D. Snyder, N. P. Hitt, B. L. Kurylyk, L. Lautz, D. J. Irvine, S. T. Hurley, and J. W.  
621 Lane. 2018. Inferring watershed hydraulics and cold-water habitat persistence using multi-year air and stream  
622 temperature signals. *Science of The Total Environment* 636:1117–1127.

623 Briggs, M. A., E. B. Voytek, F. D. Day-Lewis, D. O. Rosenberry, and J. W. Lane. 2013. Understanding Water Column  
624 and Streambed Thermal Refugia for Endangered Mussels in the Delaware River. *Environmental Science &*  
625 *Technology* 47:11423–11431.

626 Brooks, J. R., P. J. Wigington, D. L. Phillips, R. Comeleo, and R. Coulombe. 2012. Willamette River Basin surface  
627 water isoscape ( $\delta^{18}\text{O}$  and  $\delta^2\text{H}$ ): temporal changes of source water within the river. *Ecosphere* 3:art39.

628 Cadbury, S. L., D. M. Hannah, A. M. Milner, C. P. Pearson, and L. E. Brown. 2008. Stream temperature dynamics  
629 within a New Zealand glacierized river basin. *River Research and Applications* 24:68–89.

630 Carro-Calvo, L., F. Jaume-Santero, R. García-Herrera, and S. Salcedo-Sanz. 2021. k-Gaps: a novel technique for  
631 clustering incomplete climatological time series. *Theoretical and Applied Climatology* 143:447–460.

632 Casas, I., and R. Fernandez-Casal. 2019. tvReg: Time-varying Coefficient Linear Regression for Single and Multi-  
633 Equations in R. SSRN Electronic Journal.

634 Casas, I., and R. Fernandez-Casal. 2021. tvReg: Time-Varying Coefficients Linear Regression for Single and Multi-  
635 Equations.

636 Chang, H., and M. Psaris. 2013. Local landscape predictors of maximum stream temperature and thermal sensitivity  
637 in the Columbia River Basin, USA. *Science of The Total Environment* 461–462:587–600.

638 Charrad, M., N. Ghazzali, V. Boiteau, and A. Niknafs. 2014. NbClust: An R Package for Determining the Relevant  
639 Number of Clusters in a Data Set. *Journal of Statistical Software* 61:1–36.

640 Cheng, Y., B. Nijssen, G. W. Holtgrieve, and J. D. Olden. 2022. Modeling the freshwater ecological response to  
641 changes in flow and thermal regimes influenced by reservoir dynamics. *Journal of Hydrology* 608:127591.

642 Chu, C., N. E. Jones, and L. Allin. 2010. Linking the thermal regimes of streams in the Great Lakes Basin, Ontario,  
643 to landscape and climate variables: THERMAL REGIMES IN ONTARIO STREAMS. *River Research and*  
644 *Applications* 26:221–241.

645 Cline, T. J., D. E. Schindler, T. E. Walsworth, D. W. French, and P. J. Lisi. 2020. Low snowpack reduces thermal  
646 response diversity among streams across a landscape. *Limnology and Oceanography Letters* 5:254–263.

647 Cressie, N. A. C. 1993. *Statistics for Spatial Data: Cressie/Statistics*. John Wiley & Sons, Inc., Hoboken, NJ, USA.

648 Daufresne, M., and P. Boët. 2007. Climate change impacts on structure and diversity of fish communities in rivers.  
649 *Global Change Biology* 13:2467–2478.

650 De'ath, G., and K. E. Fabricius. 2000. Classification and regression trees: a powerful yet simple technique for  
651 ecological data analysis. *Ecology* 81:3178–3192.

652 Debose, A., and M. W. Klungland. 1964. Soil survey of Snohomish County area. US Department of Agriculture, Soil  
653 Conservation Service, Washington, D. C.

654 Donato, M. M. 2002. A statistical model for estimating stream temperatures in the Salmon and Clearwater River  
655 basins, Central Idaho. Water Resources Investigations Report, U.S. Geological Survey, Washington, D. C.

656 Elsner, M. M., L. Cuo, N. Voisin, J. S. Deems, A. F. Hamlet, J. A. Vano, K. E. B. Mickelson, S.-Y. Lee, and D. P.  
657 Lettenmaier. 2010. Implications of 21st century climate change for the hydrology of Washington State.  
658 *Climatic Change* 102:225–260.



659 Frizzell, V. A. 1979. Petrology and stratigraphy of Paleogene nonmarine sandstones, Cascade Range, Washington.  
660 Open-File Report, U.S. Geological Survey.

661 Garner, G., D. M. Hannah, J. P. Sadler, and H. G. Orr. 2014. River temperature regimes of England and Wales: spatial  
662 patterns, inter-annual variability and climatic sensitivity: RIVER TEMPERATURE REGIMES OF  
663 ENGLAND AND WALES. *Hydrological Processes* 28:5583–5598.

664 Gendaszek, A. S., D. M. Ely, S. R. Hinkle, S. C. Kahle, and W. B. Welch. 2014. Hydrogeologic framework and  
665 groundwater/surface-water interactions of the upper Yakima River Basin, Kittitas County, central  
666 Washington. Scientific Investigations Report, U.S. Geological Survey.

667 Georges, B., A. Michez, H. Piegay, L. Huylenbroeck, P. Lejeune, and Y. Brostaux. 2021. Which environmental factors  
668 control extreme thermal events in rivers? A multi-scale approach (Wallonia, Belgium). *PeerJ* 9:e12494.

669 Goldin, A. 1973. Soil survey of King County area, Washington. US Department of Agriculture, Soil Conservation  
670 Service, Washington, D. C.

671 Goldin, A. 1992. Soil survey of Whatcom County area, Washington. US Department of Agriculture, Soil Conservation  
672 Service, Washington, D. C.

673 Haggarty, R. A., C. A. Miller, and E. M. Scott. 2015. Spatially weighted functional clustering of river network data.  
674 *Journal of the Royal Statistical Society: Series C (Applied Statistics)* 64:491–506.

675 Hare, D. K., A. M. Helton, Z. C. Johnson, J. W. Lane, and M. A. Briggs. 2021. Continental-scale analysis of shallow  
676 and deep groundwater contributions to streams. *Nature Communications* 12:1450.

677 Hennig, C. 2020. *fpc: Flexible Procedures for Clustering*.

678 Hilderbrand, R. H., M. T. Kashiwagi, and A. P. Prochaska. 2014. Regional and Local Scale Modeling of Stream  
679 Temperatures and Spatio-Temporal Variation in Thermal Sensitivities. *Environmental Management* 54:14–  
680 22.

681 Hill, R. A., M. H. Weber, S. G. Leibowitz, A. R. Olsen, and D. J. Thornbrugh. 2016. The Stream-Catchment  
682 (StreamCat) Dataset: A Database of Watershed Metrics for the Conterminous United States. *JAWRA Journal*  
683 *of the American Water Resources Association* 52:120–128.

684 Hoover, D. 1998. Nonparametric smoothing estimates of time-varying coefficient models with longitudinal data.  
685 *Biometrika* 85:809–822.

686 Hrachowitz, M., C. Soulsby, C. Imholt, I. A. Malcolm, and D. Tetzlaff. 2010. Thermal regimes in a large upland  
687 salmon river: a simple model to identify the influence of landscape controls and climate change on maximum  
688 temperatures. *Hydrological Processes* 24:3374–3391.

689 Isaak, D. J., C. H. Luce, G. L. Chandler, D. L. Horan, and S. P. Wollrab. 2018a. Principal components of thermal  
690 regimes in mountain river networks. *Hydrology and Earth System Sciences* 22:6225–6240.

691 Isaak, D. J., C. H. Luce, D. L. Horan, G. L. Chandler, S. P. Wollrab, W. B. Dubois, and D. E. Nagel. 2020. Thermal  
692 Regimes of Perennial Rivers and Streams in the Western United States. *JAWRA Journal of the American  
693 Water Resources Association* 56:842–867.

694 Isaak, D. J., C. H. Luce, D. L. Horan, G. L. Chandler, S. P. Wollrab, and D. E. Nagel. 2018b. Global Warming of  
695 Salmon and Trout Rivers in the Northwestern U.S.: Road to Ruin or Path Through Purgatory? *Transactions  
696 of the American Fisheries Society* 147:566–587.

697 Isaak, D. J., S. J. Wenger, E. E. Peterson, J. M. Ver Hoef, D. E. Nagel, C. H. Luce, S. W. Hostetler, J. B. Dunham, B.  
698 B. Roper, S. P. Wollrab, G. L. Chandler, D. L. Horan, and S. Parkes-Payne. 2017. The NorWeST Summer  
699 Stream Temperature Model and Scenarios for the Western U.S.: A Crowd-Sourced Database and New  
700 Geospatial Tools Foster a User Community and Predict Broad Climate Warming of Rivers and Streams.  
701 *Water Resources Research* 53:9181–9205.

702 Isaak, D. J., S. Wollrab, D. Horan, and G. Chandler. 2012. Climate change effects on stream and river temperatures  
703 across the northwest U.S. from 1980–2009 and implications for salmonid fishes. *Climatic Change* 113:499–  
704 524.

705 Isaak, D. J., M. K. Young, C. H. Luce, S. W. Hostetler, S. J. Wenger, E. E. Peterson, J. M. Ver Hoef, M. C. Groce, D.  
706 L. Horan, and D. E. Nagel. 2016. Slow climate velocities of mountain streams portend their role as refugia  
707 for cold-water biodiversity. *Proceedings of the National Academy of Sciences* 113:4374–4379.

708 Jackson, F. L., R. J. Fryer, D. M. Hannah, C. P. Millar, and I. A. Malcolm. 2018. A spatio-temporal statistical model  
709 of maximum daily river temperatures to inform the management of Scotland’s Atlantic salmon rivers under  
710 climate change. *Science of The Total Environment* 612:1543–1558.

711 Johnson, S. L. 2003. Stream temperature: scaling of observations and issues for modelling. *Hydrological Processes*  
712 17:497–499.

713 Johnson, Z. C., B. G. Johnson, M. A. Briggs, C. D. Snyder, N. P. Hitt, and W. D. Devine. 2021. Heed the data gap:  
714 Guidelines for using incomplete datasets in annual stream temperature analyses. *Ecological Indicators*  
715 122:107229.

716 Johnson, Z. C., C. D. Snyder, and N. P. Hitt. 2017. Landform features and seasonal precipitation predict shallow  
717 groundwater influence on temperature in headwater streams. *Water Resources Research* 53:5788–5812.

718 Johnson, Z. C., J. J. Warwick, and R. Schumer. 2014. Factors affecting hyporheic and surface transient storage in a  
719 western U.S. river. *Journal of Hydrology* 510:325–339.

720 Jordan, C. E., and E. Fairfax. 2022. Beaver: The North American freshwater climate action plan. *WIREs Water* 9.

721 Kelleher, C. A., H. E. Golden, and S. A. Archfield. 2021. Monthly river temperature trends across the US confound  
722 annual changes. *Environmental Research Letters* 16:104006.

723 Kelleher, C., T. Wagener, M. Gooseff, B. McGlynn, K. McGuire, and L. Marshall. 2012. Investigating controls on the  
724 thermal sensitivity of Pennsylvania streams. *Hydrological Processes* 26:771–785.

725 Krzywinski, M., and N. Altman. 2017. Classification and regression trees. *Nature Methods* 14:757–758.

726 Lance, G. N., and W. T. Williams. 1967. A general theory of classificatory sorting strategies: II. Clustering systems.  
727 *The Computer Journal* 10:271–277.

728 Leach, J. A., C. Kelleher, B. L. Kurylyk, R. D. Moore, and B. T. Neilson. 2023. A primer on stream temperature  
729 processes. *WIREs Water* 10:e1643.

730 Leach, J. A., and R. D. Moore. 2019. Empirical Stream Thermal Sensitivities May Underestimate Stream Temperature  
731 Response to Climate Warming. *Water Resources Research* 55:5453–5467.

732 Li, H., X. Deng, C. A. Dolloff, and E. P. Smith. 2016. Bivariate functional data clustering: grouping streams based on  
733 a varying coefficient model of the stream water and air temperature relationship. *Environmetrics* 27:15–26.

734 Li, H., X. Deng, D.-Y. Kim, and E. P. Smith. 2014. Modeling maximum daily temperature using a varying coefficient  
735 regression model. *Water Resources Research* 50:3073–3087.

736 Li, H., X. Deng, and E. Smith. 2017. Missing data imputation for paired stream and air temperature sensor data:  
737 Missing Data Imputation for Stream and Air Temperature. *Environmetrics* 28:e2426.

738 Lisi, P. J., D. E. Schindler, T. J. Cline, M. D. Scheuerell, and P. B. Walsh. 2015. Watershed geomorphology and  
739 snowmelt control stream thermal sensitivity to air temperature. *Geophysical Research Letters* 42:3380–3388.

740 Luce, C., B. Staab, M. Kramer, S. Wenger, D. Isaak, and C. McConnell. 2014. Sensitivity of summer stream  
741 temperatures to climate variability in the Pacific Northwest. *Water Resources Research* 50:3428–3443.

742 Maheu, A., N. L. Poff, and A. St-Hilaire. 2016. A Classification of Stream Water Temperature Regimes in the  
743 Conterminous USA: Classification of Stream Temperature Regimes. *River Research and Applications*  
744 32:896–906.

745 Mantua, N., I. Tohver, and A. Hamlet. 2010. Climate change impacts on streamflow extremes and summertime stream  
746 temperature and their possible consequences for freshwater salmon habitat in Washington State. *Climatic*  
747 *Change* 102:187–223.

748 Mauger, S., R. Shaftel, J. C. Leppi, and D. J. Rinella. 2017. Summer temperature regimes in southcentral Alaska  
749 streams: watershed drivers of variation and potential implications for Pacific salmon. *Canadian Journal of*  
750 *Fisheries and Aquatic Sciences* 74:702–715.

751 Mayer, T. D. 2012. Controls of summer stream temperature in the Pacific Northwest. *Journal of Hydrology* 475:323–  
752 335.

753 McGill, L. M., J. R. Brooks, and E. A. Steel. 2021. Spatiotemporal dynamics of water sources in a mountain river  
754 basin inferred through  $\Delta^2\text{H}$  and  $\Delta^{18}\text{O}$  of water. *Hydrological Processes* 35.

755 Meier, W., C. Bonjour, A. Wüest, and P. Reichert. 2003. Modeling the Effect of Water Diversion on the Temperature  
756 of Mountain Streams. *Journal of Environmental Engineering* 129:755–764.

757 Menberg, K., P. Blum, B. L. Kurylyk, and P. Bayer. 2014. Observed groundwater temperature response to recent  
758 climate change. *Hydrology and Earth System Sciences* 18:4453–4466.

759 Mohseni, O., T. R. Erickson, and H. G. Stefan. 1999. Sensitivity of stream temperatures in the United States to air  
760 temperatures projected under a global warming scenario. *Water Resources Research* 35:3723–3733.

761 Mohseni, O., and H. G. Stefan. 1999. Stream temperature/air temperature relationship: a physical interpretation.  
762 *Journal of Hydrology* 218:128–141.

763 Mohseni, O., H. G. Stefan, and J. G. Eaton. 2003. Global Warming and Potential Changes in Fish Habitat in U.S.  
764 Streams. *Climatic Change* 59:389–409.

765 Mohseni, O., H. G. Stefan, and T. R. Erickson. 1998. A nonlinear regression model for weekly stream temperatures.  
766 *Water Resources Research* 34:2685–2692.

767 Montgomery Water Group. 2003. Wenatchee River Basin Watershed Assessment.

768 Musselman, K. N., N. Addor, J. A. Vano, and N. P. Molotch. 2021. Winter melt trends portend widespread declines  
769 in snow water resources. *Nature Climate Change* 11:418–424.

770 Neff, B. P., D. O. Rosenberry, S. G. Leibowitz, D. M. Mushet, H. E. Golden, M. C. Rains, J. R. Brooks, and C. R.  
771 Lane. 2019. A Hydrologic Landscapes Perspective on Groundwater Connectivity of Depressional Wetlands.  
772 *Water* 12:50.

773 Nelson, L. M. 1971. Sediment transport by streams in the Snohomish River basin, Washington: October 1967-  
774 June 1969.

775 O’Driscoll, M. A., and D. R. DeWalle. 2006. Stream–air temperature relations to classify stream–ground water  
776 interactions in a karst setting, central Pennsylvania, USA. *Journal of Hydrology* 329:140–153.

777 Olden, J. D., M. J. Kennard, and B. J. Pusey. 2012. A framework for hydrologic classification with a review of  
778 methodologies and applications in ecohydrology: A FRAMEWORK FOR HYDROLOGIC  
779 CLASSIFICATION. *Ecohydrology* 5:503–518.

780 Olden, J. D., J. J. Lawler, and N. L. Poff. 2008. Machine Learning Methods Without Tears: A Primer for Ecologists.  
781 *The Quarterly Review of Biology* 83:171–193.

782 Parkinson, E. A., E. V. Lea, M. A. Nelitz, J. M. Knudson, and R. D. Moore. 2016. Identifying Temperature Thresholds  
783 Associated with Fish Community Changes in British Columbia, Canada, to Support Identification of  
784 Temperature Sensitive Streams: STREAM TEMPERATURE AND FISH COMMUNITIES. *River Research  
785 and Applications* 32:330–347.

786 Patton, N. R., K. A. Lohse, S. E. Godsey, B. T. Crosby, and M. S. Seyfried. 2018. Predicting soil thickness on soil  
787 mantled hillslopes. *Nature Communications* 9:3329.

788 Pollock, M. M., T. J. Beechie, J. M. Wheaton, C. E. Jordan, N. Bouwes, N. Weber, and C. Volk. 2014. Using Beaver  
789 Dams to Restore Incised Stream Ecosystems. *BioScience* 64:279–290.

790 Pyne, M. I., and N. L. Poff. 2017. Vulnerability of stream community composition and function to projected thermal  
791 warming and hydrologic change across ecoregions in the western United States. *Global Change Biology*  
792 23:77–93.

793 R Core Team. 2020. R: A Language and Environment for Statistical Computing. R Foundation for Statistical  
794 Computing, Vienna, Austria.

795 Savoy, P., A. P. Appling, J. B. Heffernan, E. G. Stets, J. S. Read, J. W. Harvey, and E. S. Bernhardt. 2019. Metabolic  
796 rhythms in flowing waters: An approach for classifying river productivity regimes. *Limnology and*  
797 *Oceanography* 64:1835–1851.

798 Siegel, J. E., A. H. Fullerton, and C. E. Jordan. 2022. Accounting for snowpack and time-varying lags in statistical  
799 models of stream temperature. *Journal of Hydrology X* 17:100136.

800 Snyder, C. D., N. P. Hitt, and J. A. Young. 2015. Accounting for groundwater in stream fish thermal habitat responses  
801 to climate change. *Ecological Applications* 25:1397–1419.

802 Snyder, M. N., N. H. Schumaker, J. B. Dunham, M. L. Keefer, P. Leinenbach, A. Brookes, J. Palmer, J. Wu, D.  
803 Keenan, and J. L. Ebersole. 2020. Assessing contributions of cold-water refuges to reproductive migration  
804 corridor conditions for adult salmon and steelhead trout in the Columbia River, USA. *Journal of*  
805 *Ecohydraulics*:1–13.

806 Soulsby, C., P. J. Rodgers, J. Petry, D. M. Hannah, I. A. Malcolm, and S. M. Dunn. 2004. Using tracers to upscale  
807 flow path understanding in mesoscale mountainous catchments: two examples from Scotland. *Journal of*  
808 *Hydrology* 291:174–196.

809 Steel, E. A., T. J. Beechie, C. E. Torgersen, and A. H. Fullerton. 2017. Envisioning, Quantifying, and Managing  
810 Thermal Regimes on River Networks. *BioScience* 67:506–522.

811 Steel, E. A., A. Marsha, A. H. Fullerton, J. D. Olden, N. K. Larkin, S.-Y. Lee, and A. Ferguson. 2019. Thermal  
812 landscapes in a changing climate: biological implications of water temperature patterns in an extreme year.  
813 *Canadian Journal of Fisheries and Aquatic Sciences* 76:1740–1756.

814 Tague, C., M. Farrell, G. Grant, S. Lewis, and S. Rey. 2007. Hydrogeologic controls on summer stream temperatures  
815 in the McKenzie River basin, Oregon. *Hydrological Processes* 21:3288–3300.

816 Therneau, T., and B. Atkinson. 2019. rpart: Recursive Partitioning and Regression Trees.

817 Thornton, M.M., Shrestha, R., Wei, Y., Thornton, P.E., Kao, S., and Wilson, B.E. 2020. DaymetDaymet: Daily  
818 Surface Weather Data on a 1-km Grid for North America, Version 4:0 MB.

819 Turney, G. L., S. C. Kahle, and N. P. Dion. 1995. Geohydrology and ground-water quality of east King County,  
820 Washington. Water Resources Investigations Report, Prepared in cooperation with Seattle-King County  
821 Department of Health Tacoma, Washington, Washington, D. C.

822 Ver Hoef, J. M., and E. E. Peterson. 2010. A Moving Average Approach for Spatial Statistical Models of Stream  
823 Networks. *Journal of the American Statistical Association* 105:6–18.

824 van Vliet, M. T. H., W. H. P. Franssen, J. R. Yearsley, F. Ludwig, I. Haddeland, D. P. Lettenmaier, and P. Kabat.  
825 2013. Global river discharge and water temperature under climate change. *Global Environmental Change*  
826 23:450–464.

827 van Vliet, M. T. H., F. Ludwig, J. J. G. Zwolsman, G. P. Weedon, and P. Kabat. 2011. Global river temperatures and  
828 sensitivity to atmospheric warming and changes in river flow: SENSITIVITY OF GLOBAL RIVER  
829 TEMPERATURES. *Water Resources Research* 47.

830 Webb, B. W., D. M. Hannah, R. D. Moore, L. E. Brown, and F. Nobilis. 2008. Recent advances in stream and river  
831 temperature research. *Hydrological Processes* 22:902–918.

832 Webb, B. W., and F. Nobilis. 2007. Long-term changes in river temperature and the influence of climatic and  
833 hydrological factors. *Hydrological Sciences Journal* 52:74–85.

834 Webb, B. W., and Y. Zhang. 1997. SPATIAL AND SEASONAL VARIABILITY IN THE COMPONENTS OF THE  
835 RIVER HEAT BUDGET. *Hydrological Processes* 11:79–101.

836 Wildrick, L. 1979. Ground Water Flow System of the Chumstick Drainage Basin. Page 5. Washington State  
837 Department of Ecology, Olympia, WA.

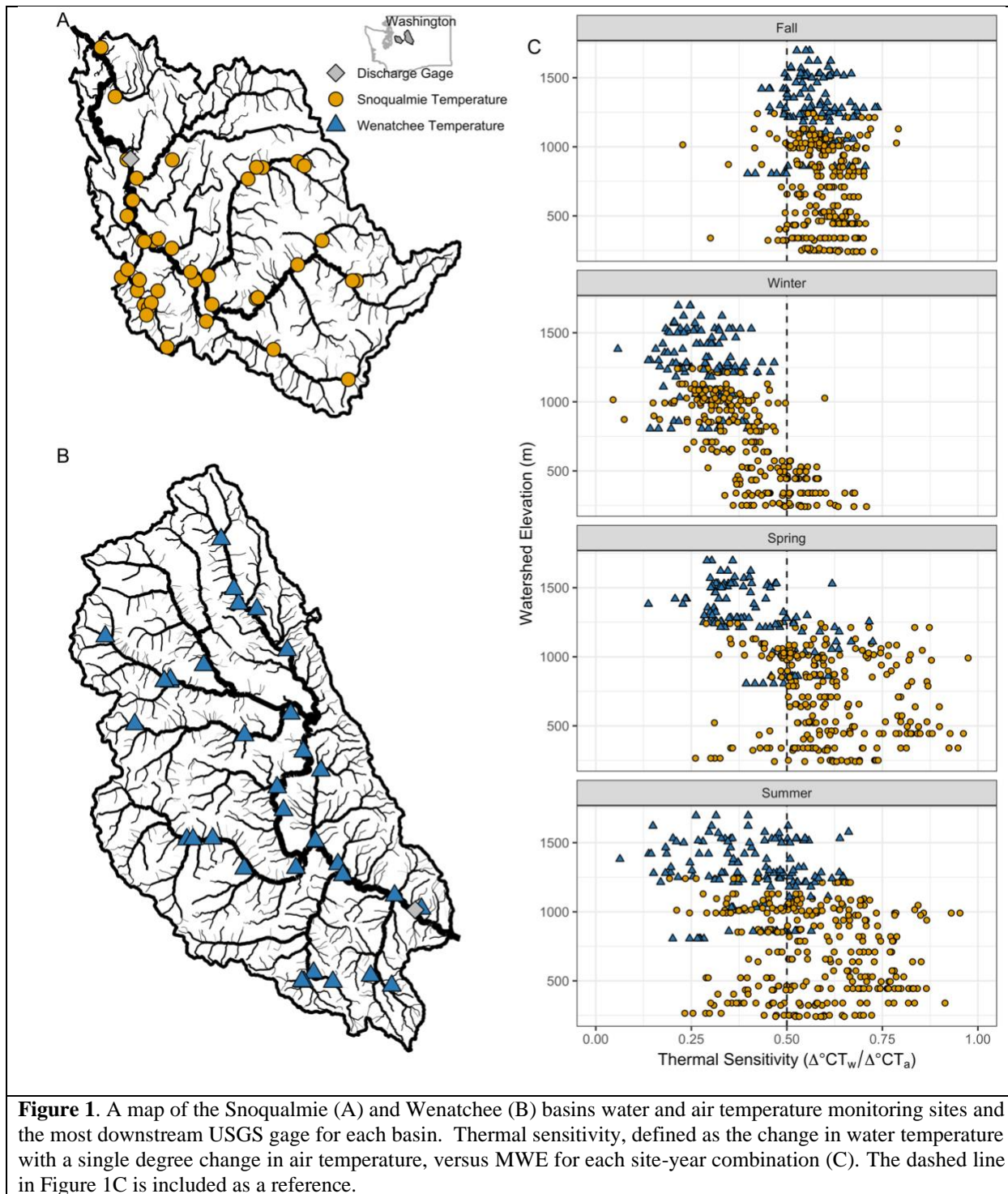
838 Winfree, M. M., E. Hood, S. L. Stuefer, D. E. Schindler, T. J. Cline, C. D. Arp, and S. Pyare. 2018. Landcover and  
839 geomorphology influence streamwater temperature sensitivity in salmon bearing watersheds in Southeast  
840 Alaska. *Environmental Research Letters* 13:064034.

841 Wolock, D. M., T. C. Winter, and G. McMahon. 2004. Delineation and Evaluation of Hydrologic-Landscape Regions  
842 in the United States Using Geographic Information System Tools and Multivariate Statistical Analyses.  
843 *Environmental Management* 34:S71–S88.

844 Wu, H., J. S. Kimball, M. M. Elsner, N. Mantua, R. F. Adler, and J. Stanford. 2012. Projected climate change impacts  
845 on the hydrology and temperature of Pacific Northwest rivers: CLIMATE CHANGE IMPACTS ON  
846 STREAMFLOW AND TEMPERATURE. *Water Resources Research* 48.

847 Yan, H., N. Sun, A. Fullerton, and M. Baerwalde. 2021. Greater vulnerability of snowmelt-fed river thermal regimes  
848 to a warming climate. *Environmental Research Letters* 16:054006.

849



850

851



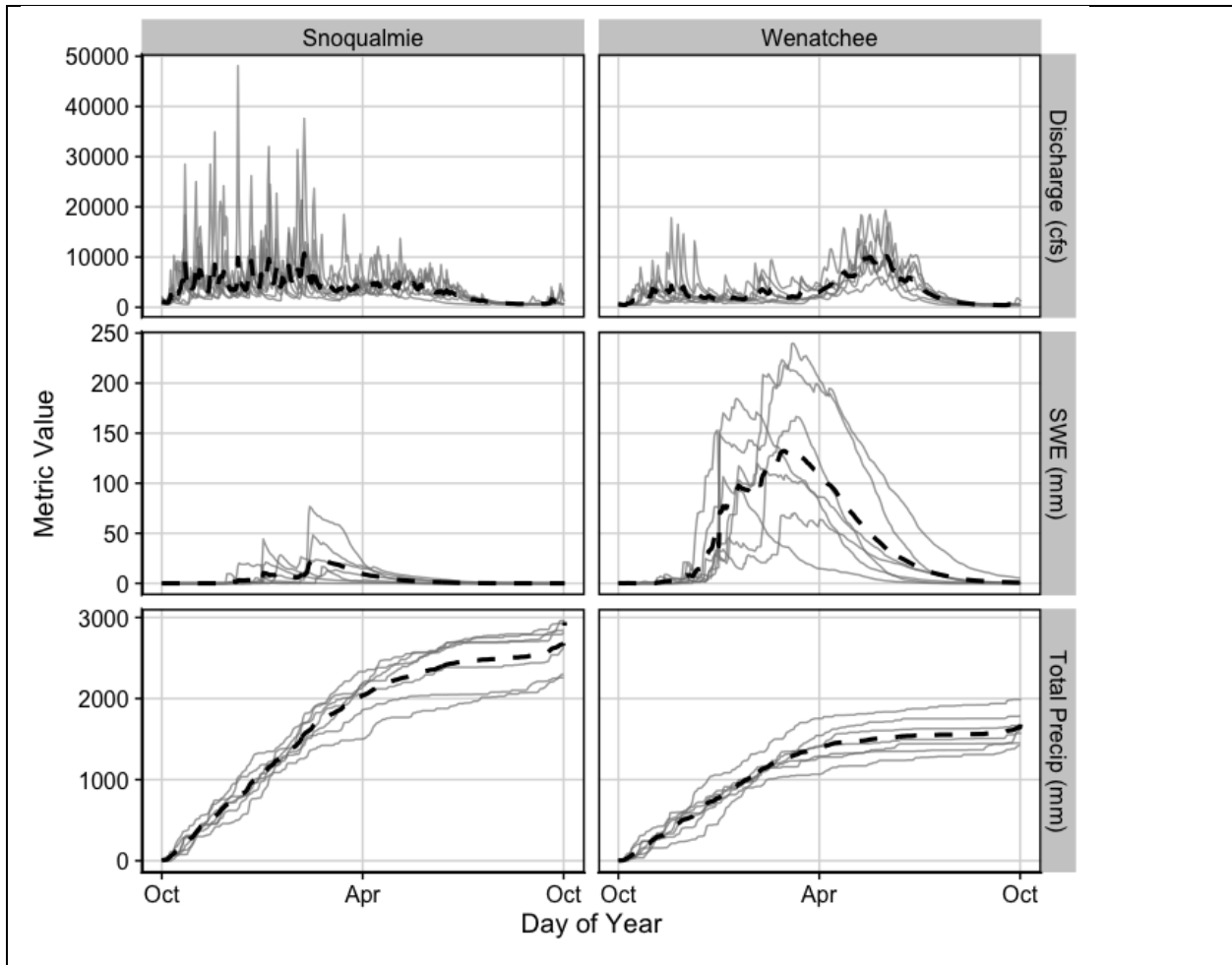


**Figure 2.** Average annual discharge, SWE, and total precipitation for the outlets of the Snoqualmie and Wenatchee basins across the sampling timeframe (black dashed lines) and interannual variability across the seven water years included in this analysis (gray lines). Discharge gage locations can be found in Figure 1A and 1B, and SWE and precipitation data is from DAYMET Daily Surface Weather data for the upstream watershed of each discharge gage (Thornton et al. 2020).

853

854

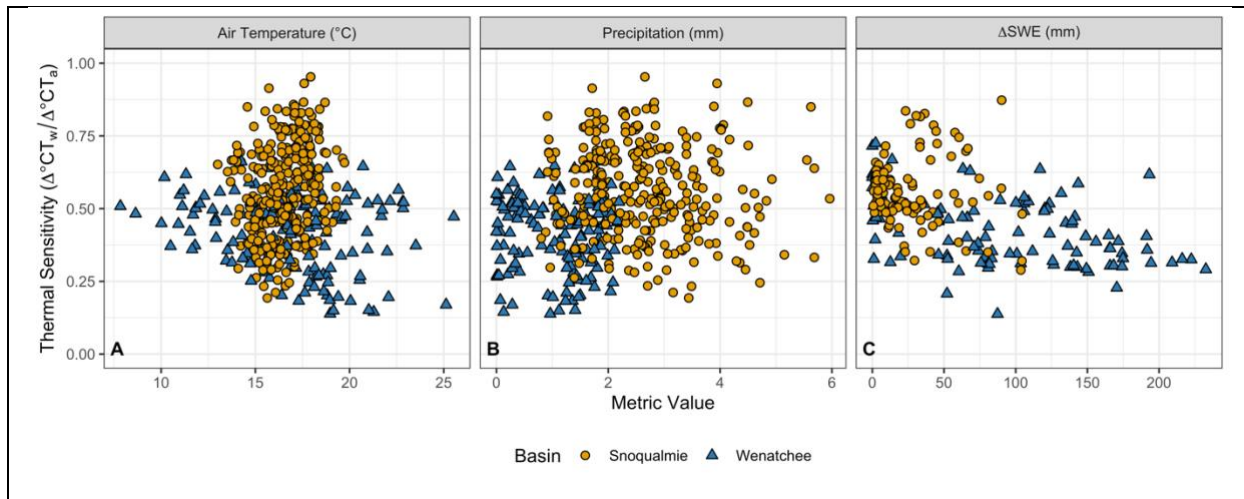


**Figure 3.** Summer thermal sensitivity values for all site-year combinations in the Snoqualmie and Wenatchee basins versus air temperature (A), and precipitation (B). Spring thermal sensitivity values for all site-year combinations versus total SWE (C) from gridded DAYMET data for each sampling point. Points are colored by basin. Basins that have no snowmelt in a given year are not shown on graph (C).

855

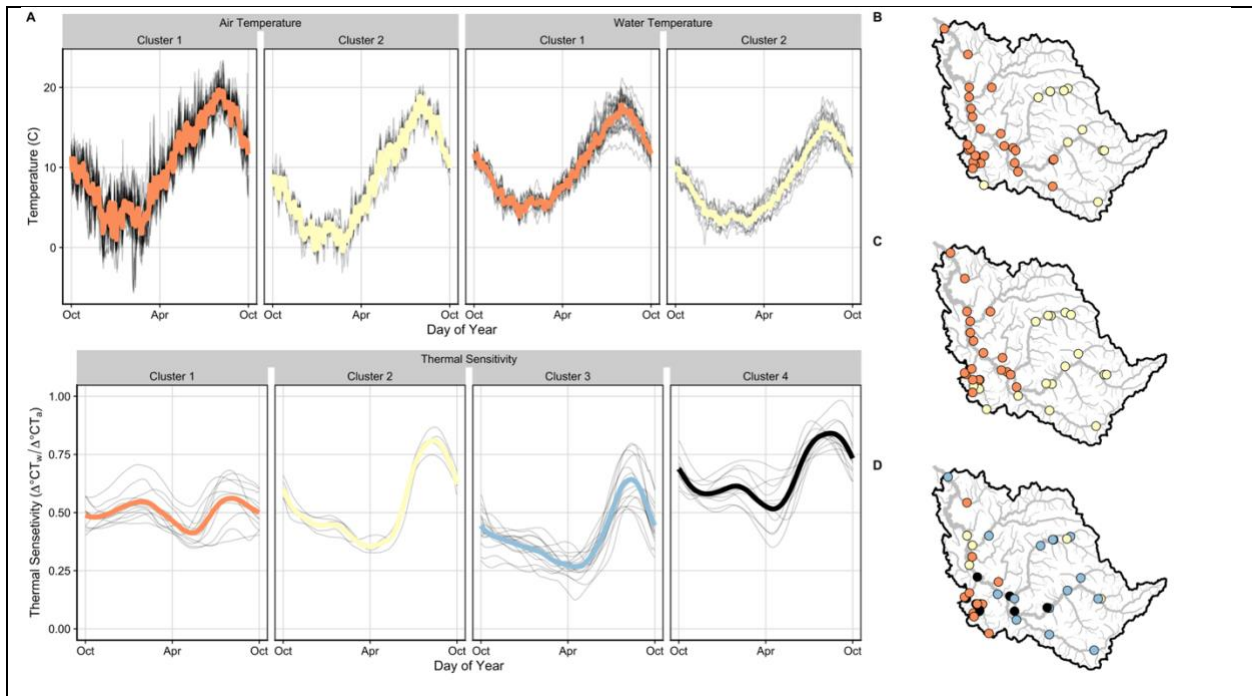


**Figure 4.** Average time series (A) and spatial clustering results (columns/colors indicate unique clusters) for average annual air temperature (B), water temperature (C), and thermal sensitivity (D) in the Snoqualmie basin. The spatial distribution for colored lines indicates mean average annual values for each cluster, and gray lines denote average annual values for each site within a given cluster.

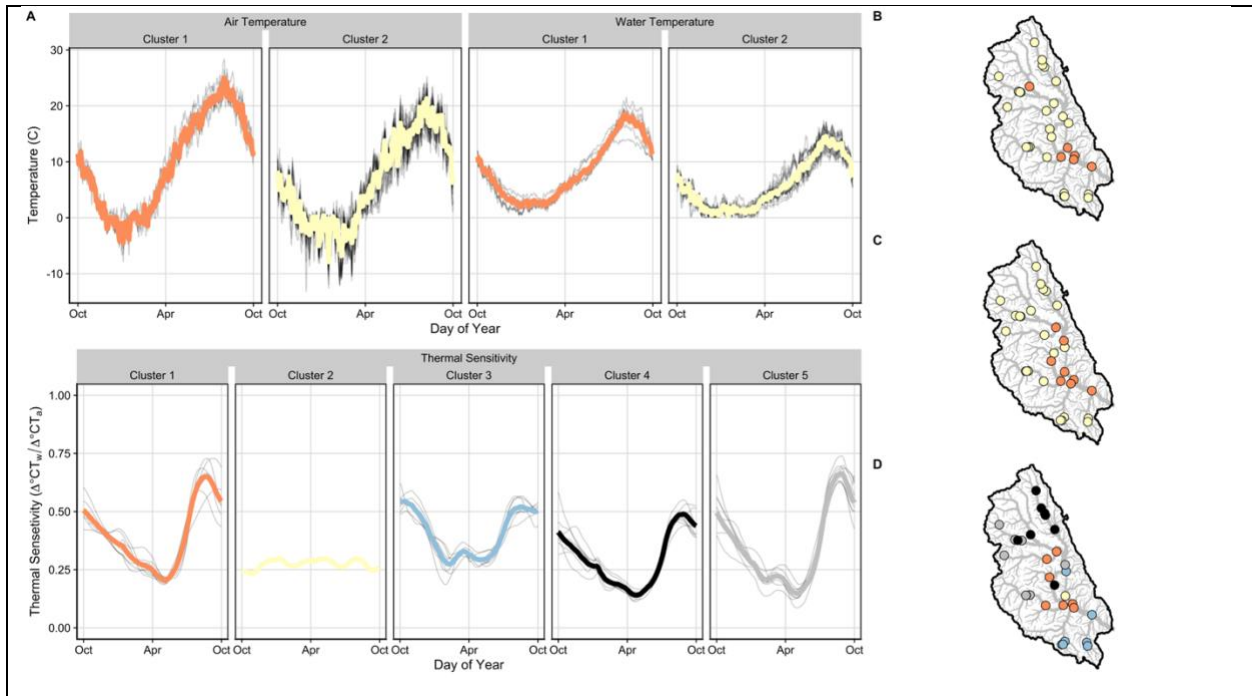


**Figure 5.** Average time series (A) and spatial clustering results (columns/colors indicate unique clusters) for average annual air temperature (B), water temperature (C), and thermal sensitivity (D) in the Wenatchee basin. The spatial distribution for colored lines indicates mean average annual values for each cluster, and gray lines denote average annual values for each site within a given cluster.

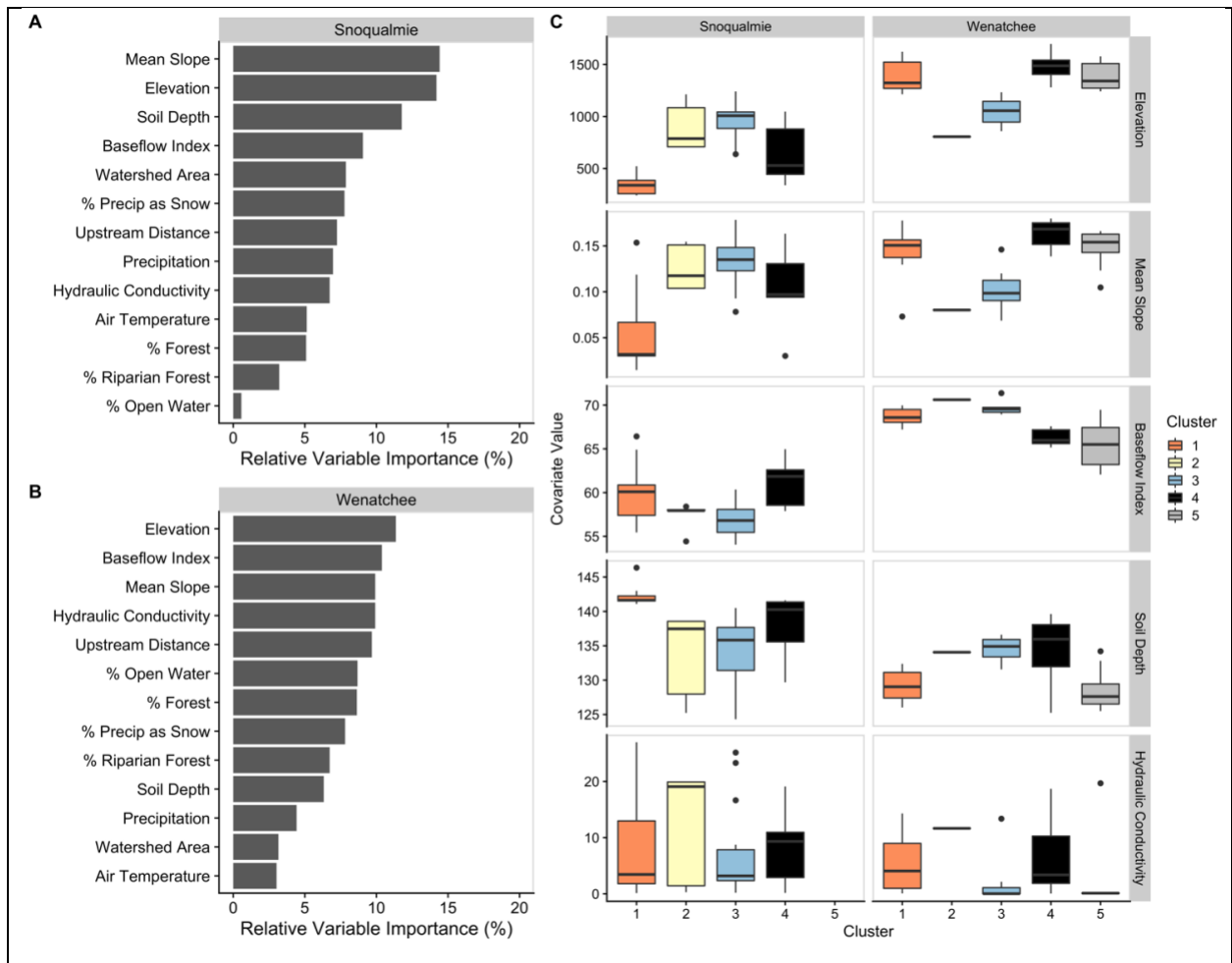


**Figure 6.** Relative variable importance for all covariates in the Snoqualmie (A) and Wenatchee (B) basins, and the distributions of variables across clusters for the four most important variables (C) in the Snoqualmie basin (Mean Slope, Elevation, Soil Depth, and Baseflow Index) and in the Wenatchee basin (Elevation, Baseflow Index, Mean Slope, and Hydraulic Conductivity). Boxes are grouped and colored by cluster membership. See Figure S8 for plots of the remaining relative variable importances.

**Table 1.** Hypothesized relationships between landscape covariates and thermal sensitivity based on previous literature (A) and the observed relationship between landscape variables and thermal sensitivities within our study basins in summer (B). Loess curves are shown to aid in visualization and correlation coefficients quantify the strength of the linear relationship. See Figure S6 for a detailed description of how river attributes covary with one another.

A. Hypothesized Drivers			B. Observed Relationship
Stream or watershed attribute (covarying variables)	Theoretical relationship with thermal sensitivity	Explanation	Observed Relationship in Summer
Mean watershed slope +elevation +dist upstream – soil depth	Negative	<ul style="list-style-type: none"> <li>Increased snowmelt and cooling due to faster velocity water movement and shorter water residence time (Winfree et al. 2018).</li> <li>Topographic shading associated with steep watersheds suppresses stream temperature by reducing exposure to solar radiation (Webb and Zhang 1997).</li> </ul>	
Mean watershed elevation +slope +dist upstream +% lake area – soil depth	Negative	<ul style="list-style-type: none"> <li>Higher elevations have higher snowmelt accumulation and greater proportion of snowmelt in spring.</li> <li>The impact of elevation on spring and early summer stream temperature is diminished in years with low winter snow accumulation.</li> </ul>	
Distance upstream – watershed size +slope +elevation	Negative	<ul style="list-style-type: none"> <li>Duration of surface water's exposure to solar radiation and atmospheric energy flux is higher in low gradient watersheds with slower streamflow velocities (Poole and Berman 2001).</li> </ul>	
Percent riparian forest cover +% forest cover – watershed size	Negative	<ul style="list-style-type: none"> <li>Riparian vegetation provides shading to streams, reducing exposure to solar radiation (Webb and Zhang 1997), particularly during summer base flows.</li> <li>Forest canopy can influence snow accumulation within a watershed and snowmelt contribution to streams. Low density forests accumulate more snow relative to</li> </ul>	

		<p>high density forests (Varhola et al 2010).</p> <ul style="list-style-type: none"> <li>• Conversion of forested land area can accelerate runoff and reduce infiltration, warming surface flows before they reach stream channels (Naiman et al. 2005; Nelson and Palmer 2007).</li> </ul>	
<p>Hydraulic Conductivity +baseflow index</p>	<p>Positive</p>	<ul style="list-style-type: none"> <li>• Hydraulic conductivity refers to the ability of a geologic material to transmit water and is calculated from mean lithological hydraulic conductivity content in surface or near surface geology.</li> <li>• Relatively high hydraulic conductivity material would be represented by something like unconsolidated alluvial sands and gravels.</li> <li>• High hydraulic conductivity is typically associated with areas of greater groundwater activity and lower, more stable thermal sensitivity values.</li> </ul>	

**Table 2.** Physical environmental data and basin characteristics used to predict air-water clusters.

Variable	Category	Units	Data Source
Watershed area	Basin Topography	km <sup>2</sup>	Hill et al. 2016
Mean watershed elevation	Basin Topography	m	Hill et al. 2016
Avg. stream slope	Basin Topography	mm <sup>-1</sup>	Hill et al. 2016
Distance upstream	Basin Topography	km	Hill et al. 2016
% Watershed forest	Land Use	%	Hill et al. 2016; Dewitz et al. 2019
% Riparian forest	Land Use	%	Hill et al. 2016; Dewitz et al. 2019
% Lake area	Land Use	%	Hill et al. 2016; Dewitz et al. 2019
Avg. Temperature	Climate	C	Thornton et al. (2020)
Avg. Precipitation	Climate	mm	Thornton et al. (2020)
Avg. % precip as snow	Climate	%	Thornton et al. (2020)
Baseflow index	Hydrogeologic	%	Hill et al. 2016; Wolock 2003
Hydraulic conductivity	Hydrogeologic	%	Hill et al. 2016; Olson and Hawkins 2014
Soil depth to bedrock	Hydrogeologic	cm	Hill et al. 2016; Carlisle et al. 2009



15 **Table 3.** Air water correlation average summary metrics by basin and season. Averages are calculated as the mean value of summary metrics at all sites across each basin and season.

		Thermal Sensitivity			R <sup>2</sup>		
		Min	Mean	Max	Min	Mean	Max
Snoqualmie	Fall	0.22	0.59	0.79	0.58	0.92	0.99
	Winter	0.05	0.40	0.71	0.20	0.86	0.96
	Spring	0.26	0.60	0.97	0.67	0.89	0.98
	Summer	0.19	0.56	0.95	0.41	0.85	0.97
Wenatchee	Fall	0.40	0.57	0.74	0.74	0.94	0.98
	Winter	0.05	0.28	0.47	0.44	0.84	0.95
	Spring	0.14	0.42	0.72	0.59	0.88	0.98
	Summer	0.06	0.41	0.66	0.08	0.77	0.96

**Table 4.** Averaged metrics for all sites within each cluster determined with the spatially weighted agglomerative hierarchical clustering. For timing metrics, days are reported as hydrologic day, where a value of 1 indicates October 1<sup>st</sup> and a value of 365 indicates September 30<sup>th</sup>.

Metric	Basin	Cluster	# Sites	Mean	Minimum (timing)	Maximum (timing)	Cluster Stability
Thermal Sensitivity	Snoqualmie	1	11	0.50	0.41 (224)	0.56 (308)	0.68
		2	5	0.52	0.36 (181)	0.81 (315)	0.88
		3	15	0.40	0.27 (201)	0.64 (316)	0.67
		4	11	0.65	0.52 (199)	0.84 (316)	0.55
	Wenatchee	1	7	0.39	0.20 (216)	0.65 (324)	0.79
		2	1	0.27	0.23 (28)	0.30 (101)	0.62
		3	7	0.40	0.27 (131)	0.54 (11)	0.94
		4	8	0.29	0.14 (207)	0.48 (331)	0.86
		5	8	0.35	0.15 (214)	0.66 (330)	0.69
	Air	Snoqualmie	1	31	10.2	1.01 (94)	19.7 (305)
2			11	8.02	-0.42 (145)	18.9 (304)	0.73
Wenatchee		1	6	9.68	-4.52 (95)	25.0 (304)	0.95
		2	25	6.48	-7.88 (107)	21.3 (310)	0.85
Water	Snoqualmie	1	25	10.1	3.91 (94)	17.8 (304)	0.65
		2	17	7.99	2.94 (94)	15.6 (304)	0.89
	Wenatchee	1	8	8.39	1.95 (108)	18.5 (310)	0.73
		2	23	5.74	0.37 (107)	14.5 (310)	0.86